MAGNETIC RESONANCE IMAGING GUIDED MUSCULOSKELETAL INTERVENTIONS AT 0.23T

Optical instrument guidance, bone biopsy, periradicular nerve root therapy, discography, osteoid osteoma laser ablation; a feasibility study

ROBERTO BLANCO SEQUEIROS

Department of Diagnostic Radiology, University of Oulu

OULU 2002

ROBERTO BLANCO SEQUEIROS

MAGNETIC RESONANCE IMAGING GUIDED MUSCULOSKELETAL INTERVENTIONS AT 0.23T

Optical instrument guidance, bone biopsy, periradicular nerve root therapy, discography, osteoid osteoma laser ablation; a feasibility study

Academic Dissertation to be presented with the assent of the Faculty of Medicine, University of Oulu, for public discussion in the Auditorium 7 of the University Hospital of Oulu, on January 24th, 2003, at 12 noon.

OULUN YLIOPISTO, OULU 2002

Supervised by
Docent Osmo Tervonen

Reviewed by
Docent Seppo Koskinen
Docent Pekka Niemi

ISBN 951-42-6903-9 (URL: http://herkules.oulu.fi/isbn9514269039/)

ALSO AVAILABLE IN PRINTED FORMAT
Acta Univ. Oul. D 708, 2002
ISBN 951-42-6902-0
ISSN 0355-3221 (URL: http://herkules.oulu.fi/issn03553221/)

OULU UNIVERSITY PRESS
OULU 2002

Blanco Sequeiros, Roberto, Magnetic resonance imaging guided musculoskeletal interventions at 0.23T. Optical instrument guidance, bone biopsy, periradicular nerve root therapy, discography, osteoid osteoma laser ablation; a feasibility study
Department of Diagnostic Radiology, University of Oulu, P.O.Box 5000, FIN-90014 University of Oulu, Finland
Oulu, Finland
2002

Abstract

The purpose of this study was firstly to evaluate the optical instrument tracking system integrated to the MRI scanner as a guidance facility in performing bone biopsy and secondly to develop and evaluate clinical musculoskeletal applications of interventional MRI at 0,23T. The clinical results and feasibility of MR-guided bone biopsy (n=14), periradicular nerve root therapy (n=61), discography (n=12) and percutaneous laser therapy of osteiod osteomas (n=5) were studied.

Bone biopsies were performed with the optical instrument tracker and bone biopsy set modified for the tracker system. The biopsy system and optical tracker mounting proved to be safe and reliable tool for bone biopsies. 14 consecutive bone biopsies and 13 fine needle aspirations were performed under MR-guidance. The clinical accuracy of MR-guided bone biopsy was 95%.

The periradicular therapy was applied to the anatomical region of lumbosacral area of 61 consecutive patients with sciatic pain. Procedural success rate was 98,5%. Of patients, 51,5% had good or excellent effect with regard to radicular pain from procedure. The therapy effect achieved with MR-guided procedure was comparable to that achieved with conventional techniques.

MR-guided discography technique and imaging protocol was developed as part of diagnostic pain provocation for patients suspected for intervertebral pain source at lumbosacral area. 34 MR-guided discographies were performed on 12 patients. In all patients positive or negative pain provocation response was obtained.

Laser induced thermal therapy for osteiod osteoma was studied in MRI. The initial guidance of the instrument and monitoring of the thermal procedure were done under MRI control. All the 5 patients were successfully treated.

The MR-guidance in musculoskeletal applications seems safe and accurate.

Keywords: bone biopsy, discography, interventional, laser therapy, magnetic resonance imaging, musculoskeletal, periradicular therapy

Para mi familia

“proceed, proceed: we will begin these rites, As we trust they’ll end in true delights”
William Shakespeare

Acknowledgements

This study was done at the Department of Radiology in the Oulu University during the years 1999-2002.

This work would not have been possible without my supervisor, docent Osmo Tervonen M.D., who has made it possible for me to conduct very fruitful research. I owe him my sincerest thanks as a supervisor and collaborator. As the professor of the Department of Radiology, Ilkka Suramo M.D., has been in key role in realizing this work from a mere vision to concrete, and I want to thank him especially for the vital notes during the last laps of the work. To Risto Ojala M.D. Ph.D., who has been my colleague both in science and other aspects of life, I want to present my deepest thanks, particularly for sharing the same vision for the art of science, which made this work so enjoyable.

I would like to express my gratitude to my co-workers Rauli Klemola M.D. and Lasse Jyrkinen Ph.D., for providing me enthusiastic conversations during the research. I also wish to thank Teuvo Vaara Ph.D. and Erkki Vahala Ph.D., for numerous last minute saves considering the manuscripts. I owe my sincerest thanks to my co-workers in other clinics and organizations, docent Ylermi Soini M.D., Elisa Lappi-Blanco M.D., Alberto Blanco Sequeiros Ph.D. and Pekka Hyvönen M.D., for invaluable assistance throughout the study.

I want thank docent Seppo Koskinen M.D. and docent Pekka Niemi M.D., for the excellent and careful review of the thesis. For the statistical analysis I want to thank Marianne Haapea M.Sc. The revision of the English language is credited to Ms. Anna Vuolteenaho.

I want express my warmest thanks to Andreas Blanco Sequeiros M.D. and Kristian Blanco Sequeiros for helping out the older brother from technological obstacles.

I express my great gratitude to all my mentors in radiology for pointing out the essence in radiology. Especially I want to thank Jaakko Karumo M.D., Ph.D and docent Seppo Lähde M.D. for leading the way.

I want to express my warmest thanks to the staff of the Departments of Interventional MRI and Northern Central Radiology for constructive attitude and help. Especially I would like to thank my colleagues Jukka Perälä M.D., Ph.D, Juho Kariniemi M.D., Matti

Isokangas M.D., docent Sami Leinonen M.D and docent Topi Siniluoto M.D. I also want to thank radiographers Kyösti Palomaa, Salme Meriläinen, Anu Kauppila and Raija Ylävaara for invaluable assistance during the study.

There are no words to describe my thanks to my parents, Guillermo and Marjatta. You have given me the heart and mind to start with.

Finally I want to express my thanks to the lights of my life, to my beloved wife Elisa, whose love never ceases to fill me with amaze and to my children, Sofia, Werner and Amanda, whose tap of little feet and general buzzing around is a fountain of happiness and never-ending stimulation for me.

Abbreviations

2D	two-dimensional
3D	three-dimensional
C-BASS	completely balanced steady state
CT	computed tomography
ESR	electron spin resonance
ETL	echo train length
EXPRESS	Philips Medical Systems acronym for SSFSE
FA	flip angle
FE	field (gradient) echo
FNA	fine needle aspiration
FOV	field of view
FSE	fast spin echo
FUS	focused ultrasound surgery
HU	Hounsfield unit
IMRI	interventional magnetic resonance imaging
IR	infra red
LITT	laser-induced thermotherapy
LoLo	local look
MR	magnetic resonance
MRI	magnetic resonance imaging
RF	radio frequency
SENSE	sensitivity encoding
SMASH	simultaneous acquisition of spatial harmonics
SNR	signal-to-noise-ratio
SSFSE	single-shot fast-spin echo
STIR	short tau inversion recovery
T	tesla
T1	longitudinal relaxation time
T2	transverse relaxation time
TA	time of acquisition
TE	time of echo

TR	time of repetition
True-FISP	fast imaging with steady-state precession
US	ultrasonography, ultrasound
XVGA	extended video graphics array

List of original publications

This thesis was based on the following articles, which are referred to in the text by their Roman numerals.

I Ojala R, Sequeiros RB, Klemola R, Vahala E, Jyrkinen L & Tervonen O (2002) MR-guided bone biopsy: preliminary report of a new guiding method. J Magn Reson Imaging 15: 82-86

II Blanco Sequeiros R, Klemola R, Ojala R, Jyrkinen L, Lappi-Blanco E, Soini Y & Tervonen O (2002) MRI-guided trephine biopsy and fine-needle aspiration in the diagnosis of bone lesions in low-field (0.23T) MRI system using optical instrument tracking. Eur Radiol 12: 830-5

III Sequeiros R, Ojala RO, Klemola R, Vaara TJ, Jyrkinen L & Tervonen OA (2002) MRI-guided periradicular nerve root infiltration therapy in low-field (0.23T) MRI-system using optical instrument tracking. Eur Radiol 12: 1331-7

IV Blanco Sequeiros R, Klemola R, Ojala R, Jyrkinen L, Vaara T & Tervonen O (2002) Percutaneous MR-guided discography in a low-field system using optical instrument tracking: a feasibility study J Magn Reson Imaging, in press

V Blanco Sequeiros R, Hyvönen P, Blanco Sequeiros A, Jyrkinen L, Ojala R, Klemola R & Tervonen O (2002) MR imaging-guided laser ablation of osteoid osteomas with use of optical instrument guidance at 0.23 Tesla. Submitted for publication.

Contents

1 Introduction

Interventional radiology was launched shortly after the discovery of X-rays. The first step was visualisation of blood vessels with angiography, followed by fluoroscopically guided biopsies and balloon angioplasties. Computed tomography (CT) and ultrasound-guided interventions emerged in the 1970s, and ultimately magnetic resonance imaging (MRI) guided interventions were introduced in the 1980s. The rapid development of interventional techniques has been led by the integration of imaging with computers, new therapy devices and operating room like conditions. This has facilitated faster and more accurate imaging and more demanding procedures have thus been applied to the repertoire of the interventional radiologist. In combining features of various other imaging modalities and adding some more to them, interventional MRI (IMRI) has potential to take further the possibilities of interventional radiology, minimally invasive therapies and surgery.

Acting as a guidance modality for interventional procedures has by no means been the birthright of MRI. The hardware has been large and clumsy for interventional use. Access to patient has been far from ergonomic and in some cases impossible. Image update frequency has been unacceptable for most interventional procedures. Strong magnetic fields and artifacts have effectively obstructed the use of interventional instruments in MRI suites. This is all very much true even today, at least when considering the older generation MRI devices. The advantages of MRI as an imaging modality have been so obvious that considerable development has taken place in the 20-year history of MRI.

The image quality has become better, ever faster software, new innovative sequences, better MRI hardware and increased computing power have accelerated imaging speed and image quality to a totally new level. Perhaps the most important feature in the recent development has been the introduction of open configuration MRI devices in the early 1990s; this enabled direct patient access and utilization of the MRI as an interventional device.

This study aimed to develop image-guided diagnostic and therapeutic musculoskeletal interventions for low field (0,23T) MRI surroundings and investigate the feasibility and clinical results of the specific musculoskeletal interventional procedures.

2 Review of the literature

2.1 Image guided interventions

Image-guided interventions to obtain diagnostic information are an integral part of evidence-based medicine. This information can be collected e.g. as bacterial, cytological and histological specimens upon pathological processes. Interventions can also be used for therapeutic purposes, much like surgery. The key concept in modern image guided procedures is minimal invasiveness, which leads to better patient compliance and often better treatment results.

The first interventional study reflecting the time to become was performed in 1896, when an angiography of a cadaver hand was obtained (Haschek & Lindenthal 1896). Angiographies on live patients were introduced during the 1920s. First image guided biopsies were performed on the 1930s as aspiration biopsies of skeletal neoplasms. Dotter and Judkins developed percutaneous transluminar angioplasty in 1964 (Dotter & Judkins 1964).

The development of ultrasound and CT boosted the use of interventional image guided procedures to a new level, -well planned, safe and effective diagnostic and therapeutic procedures were now possible. It is possible to do biopsies, aspirations, drainages, palliative tumour therapies and procedures under imaging guidance (Martino *et al*. 1984, Sones 1984, Livraghi 2001) Magnetic resonance imaging (MRI) was established as a promising diagnostic tool in the beginning of 1980s, it was soon recognized that MRI was a superior diagnostic imaging modality in diagnosing many pathological conditions and could be used for interventional procedures as a guidance method (Lufkin *et al*. 1987, Lufkin *et al*. 1988, Jolesz & Blumenfeld 1994, Lewin *et al*. 1998, Kettenbach *et al*. 2000).

2.1.1 Bone biopsy

Correct assessment of information obtainable from lesions of infectious, malignant or benign origin is essential for the selection of effective treatment in bone diseases. Although surgical biopsy is often considered the method of choice to obtain diagnosis in bone lesions, a substantial proportion (18.2%) of biopsy samples obtained at surgical biopsies may be unsatisfactorily diagnosed (Mankin *et al*. 1982). The percutaneous biopsy technique reduces the cost of the procedure, the anesthetic requirements, and the risk of complications when compared to the surgical biopsy technique (Fraser-Hill *et al*. 1992). Percutaneous biopsy is performed by inserting a trephine needle through the skin to the desired location under imaging guidance. The sample is then collected by forwarding the drill to the lesion through the trephine. The drill is then removed and a cylindrical biopsy sample is collected. Almost any location in the human body can be reached with percutaneous biopsy techniques, but the most common site for biopsies are the long bone of extremities, reflecting the distribution of bone pathology in general.

Cross-sectional imaging modalities, such as CT and MRI, are more time-consuming but provide better visualization of the bone lesion than fluoroscopy (Neuerburg *et al*. 1998a). A percutaneous approach using x-ray fluoroscopy or CT- guidance is feasible in bone biopsies, with a reported initial success rate of 97 to 100 % (Settle *et al*. 1990, Tikkakoski *et al*. 1992, Jelinek *et al*. 1996, Leffler & Chew 1999). The complication rate is low, with no reported complications (Jelinek *et al*. 1996, Leffler & Chew 1999).

2.1.2 Periradicular therapy

In selective nerve root therapy a mixture of therapeutic agents, usually a corticosteroid-anesthetics combination, is injected to the periradicular nerve root channel. This is called periradicular nerve root infiltration.

Selective periradicular nerve root infiltration with local corticosteroids and anesthetics has been used for preoperative evaluation of lumbosacral pain and sciatica patients in order to determine the not always clear correlation between the clinical symptoms and imaging findings (Krempen *et al*. 1975, Wilppula & Jussila 1977, Boden *et al*. 1990, Jensen *et al*. 1994). Periradicular nerve root infiltration has also a significant therapeutic effect in discogenic radicular lumbosacral and sciatic pain (Weiner & Fraser 1997, Lutz *et al*. 1998, Ojala *et al*. 2000, Karppinen *et al*. 2001). Weiner and Fraser reported that 78.5 % of patients with lumbar radicular pain had considerable and sustained relief from their symptoms (Weiner & Fraser 1997). In a study where CT was used as a guidance modality 55% of patients experienced excellent therapy effect free of symptoms, or had experienced some improvement when evaluated 4 months after treatment (Uhlenbrock & Arlinghaus 1997). Karppinen *et al*. reported that combined injection of anesthetic and steroid to the periradicular space resulted in at least short-term pain relief from sciatica and facilitated conservative treatment in contained herniation situation (Karppinen *et al*. 2001).

2.1.3 Discography

Discography is a minimally invasive procedure where diagnostic contrast agent is injected to an intervertebral disc to assess disc pathology and origin of the pain (Tehranzadeh 1998). It is also used as a provocative test to evaluate possible concordant pain to patients' spinal area symptoms (Weishaupt *et al*. 2001). An effective use of discography as a diagnostic tool is achieved when it is used for pre-surgical evaluation on patients considered for vertebral fusion operation (Vamvanij *et al*. 1998, Derby *et al*. 1999, Carragee 2000) .

Discography is performed under fluoroscopic control from an oblique posterior approach in the lumbar spine. The lumbar disc is punctured with a needle and diagnostic dye is injected into the disc. Sometimes a CT-study is added to obtain more information about disc characteristics after dye injection (Sachs *et al*. 1987).

Magnetic resonance imaging (MRI) is generally considered to be the most informative form of medical imaging in describing intervertebral disc degeneration and related pathology. Despite the advantages of MRI the more invasive discography is still sometimes needed to verify the location of the pain. The disadvantage of discography is the high initial radiation dose due to procedural times that are often long in fluoroscopy, especially if complemented by CT- study. MRI discography has also been reported (Huang *et al*. 2002), in this study the results indicated high concurrence between CT- and MRI-discography.

2.1.4 Laser induced bone thermotherapy of osteoid osteoma

Osteoid osteoma is a benign bone neoplasm. Its incidence has a male prevalence. The age range of patients varies from 2 to 50 years, with more than 50 % of tumors occurring before 20 years of age (Kransdorf *et al*. 1991) The typical symptoms consist of local fluctuating pain at the site of tumor, which is worse at night and dramatically improved by aspirin treatment. The radiological diagnosis is very accurate when a combination of X-ray-, CT- and/or MRI modalities is used (Greenspan 1993, Assoun *et al*. 1994, Shankman *et al*. 1997, Radcliffe *et al*. 1998, Spouge & Thain 2000, Yildiz *et al*. 2001). Together with clinical findings a high confidence imaging-based diagnosis is possible (Roger *et al*. 1996, Cerase & Priolo 1998, Sans *et al*. 1999). Traditional treatment is surgical operation and curettage of nidus with possible autologous bone patch (Campanacci *et al*. 1999). Percutanous interstitial laser treatment and radiofrequency has been successfully applied to osteoid osteoma under CT guidance (de Berg *et al*. 1995, Gangi *et al*. 1997a, Rosenthal *et al*. 1998, Barei *et al*. 2000, Cove *et al*. 2000, Witt *et al*. 2000, Lindner *et al*. 2001, Woertler *et al*. 2001).

MRI is frequently used for thermal therapy monitoring and guidance. Interstitial tumor therapy can be achieved via radiation and chemical or thermal coagulation of tissue. Brachytherapy is widely in use. Alcohol and other cytotoxic substances are frequently used (Livraghi 2001) for chemical cell destruction. Thermal coagulation in tissue can be achieved by heating the tissue with laser (Vogl *et al*. 1999a, Fiedler *et al*. 2001), radiofrequency energy (Solbiati *et al*. 2001), microwaves (Midorikawa *et al*. 2000), Cryotherapy (Neeleman *et al*. 2001) and focused ultrasound (FUS) (Hynynen *et al*. 2001, Jolesz *et al*. 2002). Depending on the indication and therapy modality used the results vary from good to excellent when compared to surgery (Jenkins *et al*. 1997, Seifert *et al*. 2000, Dick *et al*. 2002)

Laser energy has been successfully used under MRI control for thermal tumour ablation. Vogl *et al*. demonstrated a series where hepatic tumours were treated with laser tumor ablation (Vogl *et al*. 1998).

RF-energy can also be used for tumor therapy (Livraghi *et al*. 2000), although special equipment is needed with MRI (Zhang *et al*. 1998, Huppert *et al*. 2000).

Microwaves affect the tissue much in the same way as RF-energy by coagulating tissue. The affected area is smaller than in laser or RF-therapy.

Cryotherapy destroys the tissue by a freezing effect and it can be done under MR-guidance (Mala *et al*. 2001). The effect of the therapy is distributed via shattering the cell structure. The affected tissue area in cryotherapy is of the same size as in laser and RF-energy.

FUS is a unique method amongst all these methods since it is truly non-invasive since it needs no skin penetration is needed. The feasibility of FUS in breast tumor therapy has been investigated (Hynynen *et al*. 2001).

The uniting factor in percutaneous tumor therapies is the low morbidity and low mortality associated with these procedures (Vogl *et al*. 1999b, Dick *et al*. 2002). Thermal therapy is not confined to soft tissue tumours, also bone tumours can be treated (Gronemeyer *et al*. 2002). Primary success rate of over 90% has been reached without initial complications and with minimal invasiveness (Gronemeyer *et al*. 2002).

2.2 *Imaging modalities* for interventional procedures

2.2.1 X-ray fluoroscopy

As a guidance modality, X-ray fluoroscopy has been the mainstay for interventional procedures for more than 60 years. It is relatively cheap, easily adapted and based upon well-tested and reliable technology.

Fluoroscopy provides real-time control over the procedure. Both uniplanar and biplanar fluoroscopy can be used, and fluoroscopy can be combined with endoscopy, CT, US and angiography (Arthur *et al*. 2002, Tanaka *et al*. 2002). Fluoroscopy provides excellent visualization of bone structures, but soft tissue resolution is poor. When using fluoroscopy for interventional procedures the operator must rely upon secondary anatomical landmarks when targeting soft tissue lesions unless contrast is used. Contrast material is needed to visualize tubular structures with fluoroscopy (Pfirrmann *et al*. 2001). A further disadvantage of fluoroscopy is the definitive radiation exposure to the operator and the patient. The radiation dose varies according to fluoroscopy time, which again is dependent upon the procedure initialized (Vehmas 1997, McParland 1998). For instance in many cases in periradicular therapy multiple sessions are needed to obtain a satisfactory result (Narozny *et al*. 2001). Also complex anatomical structures are also difficult to figure in fluoroscopy, leading to technical difficulties in performing procedures such as sacral periradicular therapy (Viton *et al*. 1998).

2.2.2 Ultrasound

The possibilities of this sectional imaging modality for interventional use were opened when the technique for ultrasound guided percutaneous puncture was described by Holm in 1972 (Holm *et al*. 1972). With the application of the Seldinger technique to the ultrasound guided punctures the indications for US-guided procedures were broadened even further (Gronvall *et al*. 1977). Ultrasound combines a set of advantages. Ultrasound provides excellent soft tissue resolution and speed with real-time imaging added with multiplanar imaging, lack of ionizing radiation and relatively low cost. It is a very good diagnostic and interventional tool in experienced hands (Schafroth *et al*. 1987, Tang *et al*. 2002). The major disadvantage is the sensitivity to changes in echo properties of tissue and the occasional difficulty in visualizing the instrument in the tissue. Ultrasound (US) is fast and cheap and provides real-time guidance, but it has limited soft tissue contrast and visualization of structures beneath gas or bone is poor. For instance, unless extensive structural destruction is present, US can be used to merely outline the surface of the bone. However, it has also been reported that successful biopsy of bone is also possible with ultrasound with an initial success rate of 98.4% (Saifuddin *et al*. 2000).

2.2.3 Computed tomography

Since its development in early the 1970s computed tomography (CT) has been the cornerstone diagnostic tool of radiological departments. This was also reflected in the interventional applications of CT. As an end-of-the-line imaging tool CT-guidance was used in cases where other imaging modalities had failed or were not applicable. CT has proved an excellent tool in performing interventional procedures. CT has good spatial resolution, especially in bone tissue. CT allows quantification of densities of tissue, thus enabling the determination of tissue properties and further increasing the informative feed for the interventional radiologist during procedure. These properties are reflected in the good safety and efficacy of CT-guided procedures (Gangi *et al*. 1997a). The capability of interventional CT has been recently enhanced due to the development of helical and multi-detector CT. CT-fluoroscopy is possible, this enables real-time guidance in interventions and makes straight-forward and more complex procedures possible (White *et al*. 1997, Laufer *et al*. 2001). In selected indications CT has been the gold standard as an interventional radiological guidance modality (Derby *et al*. 1992, Seibel *et al*. 1997). The drawback of CT- guidance is the inherent radiation to which the operator and the patient are exposed (Silverman *et al*. 1999, Paulson *et al*. 2001, Teeuwisse *et al*. 2001) Another weakness is the ability to do real-time imaging in one plane only. Image reconstructions are possible, but these are usually time consuming and do not serve as a tool during procedure, although they are of value in procedural planning though (Wolf *et al*. 2001).

2.2.4 Magnetic resonance imaging

First interventional procedures under MRI were done in the 1980s (Mueller *et al*. 1986). They were started as aspiration biopsies and biopsies (Duckwiler *et al*. 1989). In 1988 vanSonnenberg *et al*. (vanSonnenberg *et al*. 1988) described a system for MR-guided biopsy and drainage. Experimental MR-guided therapies were reported in 1992 by Cline *et al*. and Matsumoto *et al*. (Cline *et al*. 1992, Matsumoto *et al*. 1992) The applications and indications of MR-guided interventions have increased steadily.

MRI interventions are done in both high field (Salomonowitz 2001) and low field devices (Popowski *et al*. 2000). The scanners are usually of closed or open type, depending of their structural and functional properties. Typically high field devices are closed bore magnets since the stronger magnetic field requires more robust shielding and gradient structure to maintain field homogeneity. The advantage of higher magnetic field is reflected in better spatial and temporal resolution. The high field scanners field strength is typically 1.5 T and above. Low field scanners are less resolute upon structural configuration of the magnet, thus it has been possible to construct open configuration MRI scanners on which one side is usually open for patient access. Scanners of this type are obviously more suited to a bed-side type interventional procedures than closed systems (Gronemeyer *et al*. 1991, Schenck *et al*. 1995). The open magnet's field strength varies from 0.2 to 1.0 T. There is trade-off in image quality towards less resolution due to open structure of these systems. The image quality of low field scanners is however quite sufficient for interventional use (Ojala *et al*. 2000, Ojala *et al*. 2001)

There are overall numerous facts that support the use of MRI in interventions. The lack of ionizing radiation is considered an important advantage; this alone may lead to the increased use of MRI in interventions in future. But there are further advantages to the MRI and these are not easily, if at all, matched by any other imaging modality; firstly, MRI provides relatively good spatial and temporal resolution (Jager & Reiser 2001). Secondly, high intrinsic contrast in tissue without or with the use of contrast medium (Tung & Davis 1993). Thirdly, multiplanar imaging capability with optional two and three-dimensional view (Murphy & Totty 1986). Furthermore, MRI has the ability to measure and quantify flow, diffusion and perfusion (Morvan *et al*. 1993, Rordorf *et al*. 1998, Pedersen *et al*. 2002). An important feature is also the temperature sensitivity of MRI, which allows the assessment of temperature changes (Quesson *et al*. 2000). Qualities of different modalities used for guidance in interventions are demonstrated in Table 1.

Table 1. Qualities of different imaging methods in interventional use.

Method	Advantages	Disadvantages
US	Easy availability	Variable spatial and contrast resolution
	No radiation	
	Low cost	Poor imaging of bone and air-filled space
	Real-time	
	Easy access to patient	
Fluoroscopy	Real-time	Ionizing radiation
	Bone imaging	Single projection
		Poor soft tissue resolution
CT	Excellent spatial and temporal capability	Limited multiplanar capability
		Not sensitive to temperature
		Limited access to patient
	Stereotactics available	Ionizing radiation
MRI (closed system)	Excellent soft tissue resolution	High cost
	Sensitive to flow, diffusion and temperature	No access to patient during imaging
MRI (open system)	Good access to patient	High cost
	Multiplanar imaging	Availability
	Good soft tissue resolution	Limited field strength
	Sensitive to Temperature	
	No ionizing radiation	

In addition, the new open configuration MRI devices are equipped with sophisticated instrument localization and user interface tools (Vahala *et al*. 2001) to facilitate almost all interventional procedures to be performed with real-time control.

The frequent clinical interventional application in MRI is biopsy. This is to be expected, since surgical biopsy is being replaced by the less invasive but equally effective image-guided percutaneous biopsy techniques in many indications (Tikkakoski *et al*. 1992, Smyczek-Gargya *et al*. 2002). The common indication for surgical biopsy is the difficult anatomical location of pathology, which makes image-guided procedure difficult to control in terms of visualizing the lesion or the surrounding structures during procedure. MRI imaging can provide unique visualization of anatomy and pathology. MRI can thus serve as potential imaging method in performing diagnostic biopsies. It seems that MRI is as effective as an imaging guidance tool as any other modality in performing biopsies (Heywang-Kobrunner *et al*. 1999, Perlet *et al*. 2002).

There are reports in which MRI's value in performing bone biopsies is advocated (Neuerburg *et al*. 1998b, Adam *et al*. 1999, Genant *et al*. 2002).

MRI can be used as a guidance tool in percutaneous drainage procedures. The advantages of using MRI in drainage procedure guidance is that MR-guidance enables oblique acute angle approach to the lesion, allows visualization of the total needle path in the same image slice during puncture, good anatomical resolution and can be used as drainage guidance modality when other guidance methods fail (Buecker *et al*. 2001) or are not available.

MR imaging in interventional procedures combines the advantages of MRI and enables to identify pain source by local injections (Mink *et al*. 1998). There are reports suggesting that in therapeutic injections MR-guidance is of value (Seibel *et al*. 1997).

Image guided tumor therapies are a wide entity with lots of applications. There are numerous possibilities for interventionalists to use both in imaging modalities and therapy modes. As an imaging modality MRI has the widest range of qualities, which makes MRI the most interesting modality to be used for therapy planning and guidance. MR-guidance has been successfully applied in interstitial laser treatment guidance and monitoring of soft tissue tumor ablation (Adam *et al*. 1999, de Jode *et al*. 1999, Vogl *et al*. 1999b, Law & Regan 2000, Fiedler *et al*. 2001).

Optimization of thermal therapies demands methods measuring temperature *in vivo* during therapy. In this respect MRI provides interesting and unique potential to measure thermal deposition in tissue during thermal treatment. This can be achieved by using different MRI techniques suitable for the purpose: T1 relaxation time of water protons, molecular diffusion constant of water, water proton resonance frequency, Proton spectroscopic imaging, temperature sensitive contrast agents, and theoretically even spin density or magnetization transfer can namely be used for MRI thermometry (Quesson *et al*. 2002).

2.2.5 Instrument tracking in interventional procedures in MRI

Instrument tracking in MRI is based upon creative use of scanner hardware, software, sequences and tracking options (Smits *et al*. 1999, Konings *et al*. 2001). MRI interventions can be performed in a straightforward diagnostic MRI unit with standard software, but it is much more feasible and also safer to perform them using user interface designed for MRI interventions (Hinks *et al*. 1998, Yrjana *et al*. 2002) (Jyrkinen *et al*. 2000). This type a software allows planning, imaging and performing the interventional procedure in a predetermined way using default settings for imaging and image windowing. This allows categorizing the interventions and providing custom-made imaging features for each of them. The software usually comes with hardware that enables monitoring the procedure from the imaging room and user interface hardware that can be used in MRI environment.

Imaging sequences in interventional MRI (IMRI) are somewhat different from the ones used in diagnostic MRI. This is due to the fact that fast imaging speed is related to good spatial and temporal resolution. It is difficult to achieve all these simultaneously; there is trade-off between image speed, signal to noise ratio, and resolution (Busch *et al*. 1998). Therefore almost all the sequences used in IMRI are custom-made and originate from fast imaging sequences. These include various gradient echo techniques generally with short TR; also different strategies for k-space sampling have been developed in order to speed up the imaging. These include LoLo (Buecker *et al*. 1998), keyhole (Duerk *et al*. 1996), segmented k-space (Heid *et al*. 1995) and wavelet encoded data acquisition techniques (Wendt *et al*. 1998). New techniques like SMASH and SENSE are likely to set the standard for image quality in coming years (Sodickson *et al*. 1999, Weiger *et al*. 2002).

Instrument tracking gives the possibility to obtain images in the instrument plane simultaneously during the procedure. This leads to a multiplanar interactive scanning environment, where the ability to interactively localize, plan and monitor the procedure is an essential feature. This kind of setting requires active instrument tracking. Active instrument tracking can be achieved in at least two ways; the instrument can be tracked with infrared camera when an appropriate number of mirrors with known locale is provided (Vahala *et al*. 2001). Other method to achieve active tracking is to use a built-in receiver or active coils in the instrument to achieve exact positional information of the device (Ladd *et al*. 1998, Joensuu *et al*. 2000). Locally induced field inhomogenities can also be used to pinpoint the instrument position (Glowinski *et al*. 1998). In this method a current is applied through a wire built in the wall of the instrument causing field inhomogeneity and thus signal void. There are also other potential methods for active instrument tracking, such as using electron spin resonance (ESR) (Ehnholm *et al*. 1999), or inducing a signal from the instrument tip from an external source (Konings *et al*. 2001).

Ideally IMRI procedures would be performed in real time imaging setting and thus simple passive instrument tracking would be sufficient; this is also an option when immediate image update is not necessary due to the nature of the procedure. Passive instrument tracking is based on the inherent susceptibility artifact caused by the instrument in the image data also this can be enhanced with modified catheter structure (Bakker *et al*. 1996). At the moment passive tracking methods are in frequent clinical use, namely instrument artifacts follow-up (Adam *et al*. 1999, Salomonowitz *et al*. 2000). Of active tracking methods, optical tracking is clinically in use (Jolesz 1998, Ojala *et al*. 2000).

2.2.6 Implications for this study

Intreventional procedures are in effect minimally invasive procedures of surgical nature. These procedures have been performed a under cluster of radiological imaging modalities, of which most recent is MRI. There are various MRI systems in use in which MRI's feasibility as a potential platform for interventional procedures has been demonstrated. Low field MRI scanner and open configuration high-field scanners seem to be most suitable for interventional procedures, but there is lack of clinical studies demonstrating the clinical feasibility of MR-guidance in interventional procedures. The information available upon procedural strategies and indications for MRI interventions is limited. The procedural instrument guidance methods are still being developed. There have been no procedural reports of MR-guided bone biopsy with associated fine needle biopsy available. Neither are any studies available with statistical results upon MR-guided nerve root therapies. Discography procedure has not been performed in low-field MRI surroundings. Thermal therapies are being increasingly used for tumor palliation and treatment; this is also being done under MR-guidance.

3 Purpose of the study

The purpose of this study was:

1. To study the feasibility of optical guidance method in conjunction with MR-guidance in bone biopsies at 0.23T.
2. To investigate clinical feasibility of MR-guidance in performing bone biopsies at 0.23T.
3. To evaluate MR-guided nerve root therapies at 0.23T.
4. To study feasibility of MR-guidance in performing discography.
5. To explore the feasibility of MR-guided thermal laser therapy in treating osteoid osteoma at 0.23T.

4 Materials and methods

4.1 Patients and procedures

The total number of patients included to these studies was 97. Bone biopsies were performed in five patients with the optical instrument tracker and bone biopsy set modified for the tracker system. The sequel study consisted of clinical experiment of 14 consecutive bone biopsies (n=14), and 13 fine needle aspirations performed under MR-guidance.

Periradicular nerve root infiltration therapy was performed on 61 consecutive patients (n=61), with sciatic pain. The periradicular therapy was applied to the anatomical region of the lumbosacral area.

MR-guided discography was performed as part of diagnostic pain provocation for patients suspected of intervertebral pain source at lumbosacral area. 34 MR-guided discographies were performed on 12 patients (n=12). Laser induced thermal therapy for osteiod osteoma therapy was applied under MR-guidance. 5 patients were treated (n=5). Informed consent was obtained from all patients. All the studies were accepted by the ethical committee of Oulu University Hospital.

4.1.1 MRI-system for interventional procedures

All the procedures were performed in the interventional MRI system which consisted of a low field MRI scanner, in-room monitor, in-room workstation with imaging capability, infra-red camera, fixed infra-red mirrors and a foot pedal for the operator which controlled sequence start. MRI scanner used was a resistive 0.23 T open configuration (C-shaped) MRI with interventional optical tracking equipment and software (Outlook Proview, Philips Medical Systems, MR Technologies Finland) (Figure 1), which was installed into a full-scale operating room. The open configuration construction with one pillar supporting the scanner allows wide passage to the patient through a 44 cm diameter horizontal gap.

Fig. 1. An open interventional MRI system.

A surface coil was used for imaging in all patients during procedure. (Figure 2). This figure also demonstrates the typical position of the patient for vertebral column area procedure.

Fig. 2. Typical set-up for musculoskeletal procedure.

The interventional MRI (IMRI) package consisted of an MR-compatible in-room console, a large-screen (36") display, optical navigator hardware, and IMRI software. The display uses a projector integrated with a backlit screen. It is capable of showing four to six images with XVGA_resolution at a viewing distance of 2–4 m. The tracking was performed with an infrared navigator camera. The camera detects two infrared-reflective trackers simultaneously, one of which is attached to the instrument and the other to the magnet pole-piece, which thereby provides a fixed reference frame.

The navigator camera is placed on an adjustable and movable stand. The camera utilizes infrared (IR) passive tracking, whereby the position of the instrument being observed is calculated from the IR pulses reflected from the spheres attached rigidly to the bone biopsy set. The camera is capable of differentiating between instrument types based on the geometrically unique configurations of the spheres on the instruments. The fixed reference frame attached to the upper pole-piece of the magnet allows repositioning of the camera during the operation, in case the line-of-sight to the needle holder becomes blocked.

The software supports instrument-guided imaging, so that the image set centre follows the instrument tip and the image plane follows the instrument orientation. The navigation software communicates with the scanner in real time, allowing real-time changes in the image plane. The default image planes were typically set in three orthogonal planes in relation to the instrument axis. Imaging can also be assessed in fixed plane mode where the relation of imaging plane to the operator is fixed. Alternatively imaging in relation to the magnetic field co-ordinates can be assessed. Alternate types of sequences with a variable number of slices (1-9 slices typically) can be assessed from preset values. The instrument dimensions were calibrated with tracking software before the puncture. The instrument and its trajectory shows as a real-time graphic overlay in the image or in the image set during procedure. The guidance software allows determination of the target as a graphic overlay item (target-point) and also provides spatial feedback from instruments position as a graphic overlay in relation to the determined target-point. The instrument was connected to the optical tracking system with a wireless instrument holder (Figure 3).

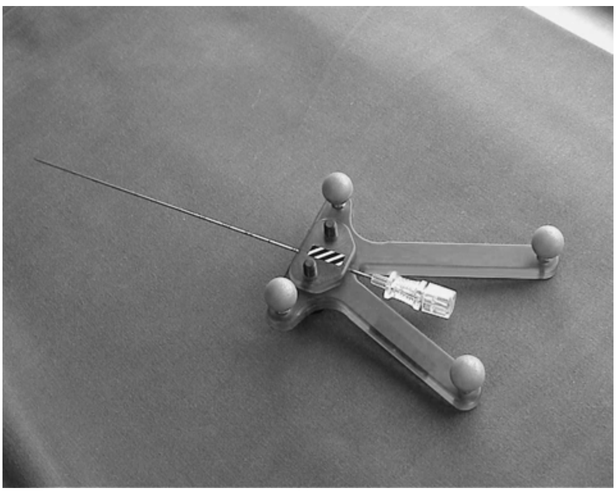

Fig. 3. Instrument holder with optical tracking system.

It is a sterilizable tool made of biocompatible plastic and equipped with infrared reflecting spheres suited for optical tracking. The holder is part of the interventional MRI package (*i*Path 200) provided by the magnet (Proview) manufacturer (Outlook Proview, Philips Medical Systems, MR Technologies Finland).

4.1.2 Procedural set-up

Before the MR-guided procedure, all the necessary precautions ensuring normal sterile and safe conditions for a procedure were performed. This included the special safety issues concerning MRI surroundings. When starting the procedure the possible site of skin puncture and procedural route was determined by means of optical tracking. This was done by placing the instrument mounted to tracker close to the skin at the supposed area of containing the lesion and taking image sets to obtain information about the procedure area and the route.

As a novel sequence to the used scanner type, CBASS (completely balanced steady state) was applied in four of the five studies. CBASS is in essence a true-FISP type sequence combining T2 and T1 expression based on the T2/T1 balance in high using high flip angles (Duerk *et al*. 1998). The composition of the sequence is demonstrated (Figure 4).

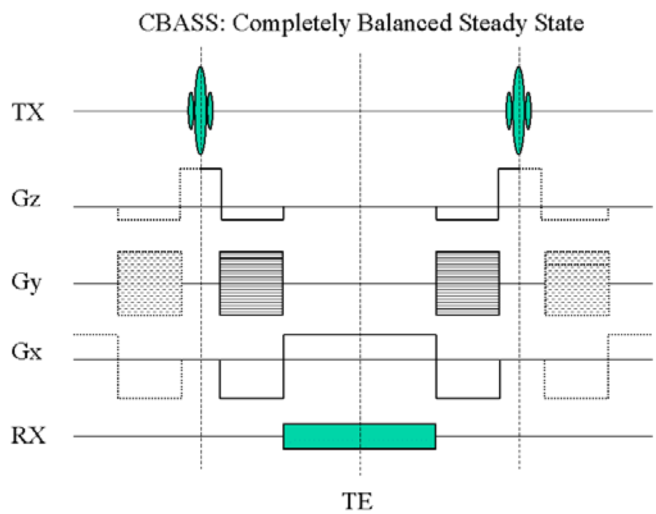

Fig. 4. CBASS (completely balanced steady state), i.e. True-FISP sequence. The composition.

This sequence is fast and allows high resolution compared to other fast imaging sequences used in low-field interventional MRI.

4.2 Guidance method for MR-guided bone biopsy

The biopsies were performed using a bone biopsy set, connected to an optical tracking system. An MR-compatible bone biopsy set ($BoneBiopsy_{TM}$, Daum GmbH, Germany) with two different drill bits (∅ 3 and 6 mm) was designed in our institution to be connected with an optical tracking system (Figure 5).

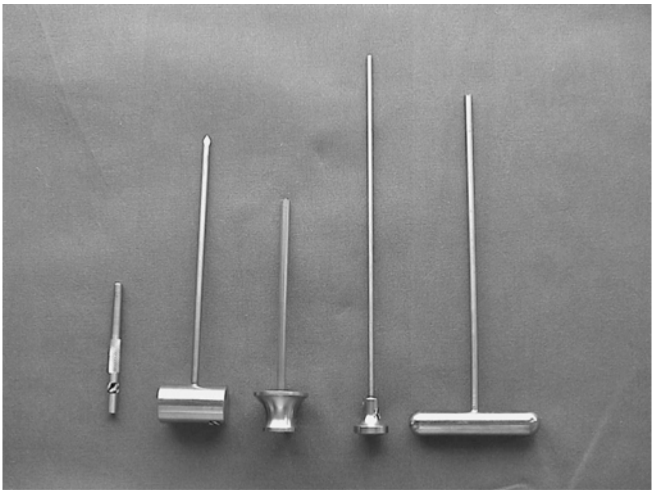

Fig. 5. MRI compatible bone biopsy set.

All parts of the set were made of a special titanium alloy, which permits the usage in MRI up to 1.5 Tesla. Because the titanium alloy is softer than stainless steel, special teeth that allow rotational drilling without axial pressure were created. The patented surface treatment of the cannulas provided safe clinical use.

The feasibility of the tracking system was evaluated with biopsies of five different anatomical areas (Table 2).

Table 2. Site, Size and final Diagnosis of Bone Lesions.

Patient	Site	Size (mm)	Diagnosis
21 y Female	Th7[a]	25	Infection
35 y Male	Femoral head	9	Fibrosis
73 y Female	Sacrum	50	Plasmocytoma
31 y Male	L5[b]	31	Lymphoma
70 y Female	Femur	15	Metastasis

[a] Seventh thoracic vertebra. [b] Fifth lumbar vertebra.

There was a total of 5 patients, 3 males and 2 males, mean age was 26 years. All the patients had had a bone lesion detected in previous plain film radiography (1 patient), CT (3 patients) or MRI (1 patient). Only one of the lesions (patient 1, table 1) was clearly seen in plain film radiography, while CT showed 3 out of 4 lesions imaged with CT. The sizes of the lesions varied from 9 to 50 mm (mean 26 mm). Two of the lesions were in the spine, one in the sacral bone, one in the femoral head and one in the femoral diaphysis. A previous malignancy was known in one patient. Two biopsies were performed under general anesthesia and three under spinal anesthesia.

Preoperatively, the lesion and the puncture route were visualized with T1-weighted fast spin echo (FSE; TR/TE 400/16 ms, echo train length (ETL) 4, flip angle (FA) 90, field of view (FOV) 380 mm x 380 mm, acquisition matrix 324 x 324, 7-mm slices, time of acquisition (TA) 22 s, number of slices 5) in a longitudinal, either sagittal or coronal, plane, depending on the anatomical area. The following needle guidance sequences were used: 1. T1-weighted gradient echo (TR/TE 95/7, ETL 1, FA 60, FOV 380 x 380, matrix 300 x 300, 7-mm slices, TA 18 s/5 slices), 2. CBASS 2D (completely balanced steady state sequence) (TR/TE 9.1/4.5, ETL 1, FA 60, FOV 380 x 380, matrix 216 x 216, 10-mm slice, TA 2 s / one slice) and 3. CBASS 3D (TR/TE 8.4/4.2, ETL 1, FA 45, FOV 380 x 380, matrix 256 x 256, 5-mm slices, TA 24 s/8 slices). The biopsies were targeted to the enhancing part of the tumor, if one had been present in the previous MRI. When the lesion's border was reached, the puncture needle was removed and a trephine bore was introduced through a trocar. The bore was then drilled into the lesion, and a sample was removed and fixed in 10% formalin. The patients remained in hospital for 24 hours for routine follow-up.

4.3 MR-guided bone biopsy

All consecutive patients referred for bone biopsy at our institution during September 1 1999- September 1 2000 were included in the study. The series consisted of 14 patients, who underwent altogether 20 percutaneous bone biopsies. 19 MR-guided trephine biopsy samples from 13 patients were collected. On 4 patients double trephine biopsy was performed during one session, on one patient triple trephine biopsy was done during one session.

In combination with MR-guided trephine biopsy thirteen FNAs targeted to the lesion area were performed on 13 patients. FNA was performed through the trochar from the channel drilled to the bone with trephine as a complementary procedure. Additional bacterial samples were aspirated in 4 cases to establish possible microbiological involvement in the lesion. A MRI compatible 20 gauge needle (MReye, Cook, Bloomington, IN, USA) was used in FNA and in aspiration for bacterial stains. Eight patients were biopsied under general anesthesia, and 6 biopsies were made under spinal anesthesia.

The mean age of the patients was 50 years (6 males, 8 females). All the patients had had a bone lesion detected in a previous radiographic, CT or MRI examination. The indications for bone biopsy were: bone lesion of unknown origin n= 5, suspected osteomyelitis n=2, suspected primary malignancy n=2, suspected metastatic lesion n=5. The bone lesion was suspected of being either neoplastic or infectious in nature. In cases with suspected osteomyelitis there was no preprocedural evidence of extraosseus infectious agent. The lesion size varied from 0.7 cm to 12 cm the mean being 3.4 cm.

The locations of the lesions were: pelvis n=4, femur n=4, lumbar spine n=2, thoracic spine n=3, tibia n=1. The lesions were graded by preoperative imaging being edematous n=7, destructive n=5 or sclerotic n=2 of nature. Lesion sizes and localizations are demonstrated in Table 3.

Table 3. Bone biopsy lesion sizes, localization and diagnosis.

Patient	Lesion size	Lesion location	Diagnosis
44 y Female	1 cm	Femur	Infection
59 y Female	2 cm	Femur	Carcinoma
31 y Male	4 cm	L5 [a]	Lymphoma
64 y Male	1 cm	Ileum	Lymphoma
67 y Male	1 cm	Ileum	Myeloma
42 y Male	3 cm	Tibia	Paget disease
21 y Female	3 cm	Th 7 [b]	Infection
32 y Female	3 cm	Th 12 [c]	Normal
35 y Male	0.7 cm	Femur	Fibrosis
56 y* Female	3 cm	Th 7 [b]	Infection
72 y Male	12 cm	Sacrum	Infection
73 y Female	4 cm	Sacrum	Fibrosis
78 y Female	4 cm	L4 [d]	Post-infection
31 y Female	3 cm	Femur	Normal

[a] Lumbar vertebra 5. [b] Thoracic vertebra 7. [c] Thoracic vertebra 12. [d] Lumbar vertebra 4. * Biopsied after transition in CT.

Two similar MRI compatible trephine biopsy sets of different caliber (inner diameter 3mm and 6 mm, Daum medical, Schwerin, Germany) with optical tracking equipment were used. The biopsy sets were modified to house a tracking tool (Figure 6).

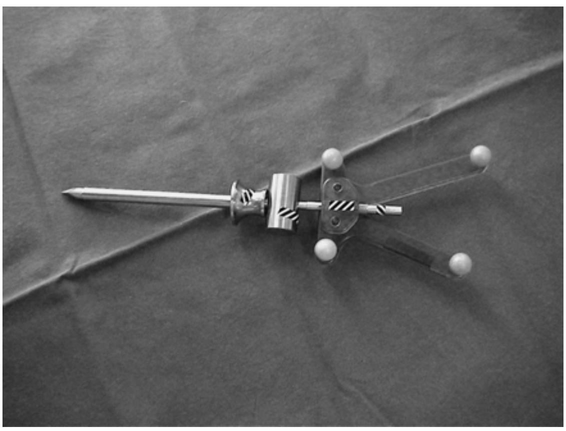

Fig. 6. Bone biopsy set with optical tracker housing.

A prerequisite for the procedure was a free route to the lesion. The route was determined with T1-weighted fast spin echo imaging (5 slices, FSE, TE 400 ms, TR 16 ms, slice thickness/ interval 7,0 mm/ 8.0 mm, FOV 380x380, matrix 324x324, acquisition time 23 seconds), CBASS imaging (8 slices, CBASS, TR 8.4 ms, TE 4.2 ms, slice thickness/ interval 5.0 mm/ 5.0 mm, FOV 380x380, matrix 256x256, acquisition time 24 seconds), and T2-weighted fast spin echo images (9 slices, FSE, TE 3500 ms, TR 150 ms, slice thickness/interval 7,0 mm/8,0 mm, FOV 380x380, matrix 192x192, acquisition time 35 seconds), were also obtained whenever no previous MRI imaging had been made. A representative, and most probably, viable part of the lesion was selected as a target. The parts of the lesion that represented extraosseous tissue extension or were not covered by cortical or osteosclerotic bone were preferred for biopsy.

The set-up for biopsy is demonstrated in Figure 2.

To reduce post-procedural pain in patients who underwent the procedure under general anesthesia, local anesthetic was then injected into the soft tissue and to the puncture route. A small skin incision was made to facilitate the initial introduction of the bone biopsy set. The biopsy needle, including the stylet and the trochar, were then advanced to the edge of the lesion using graphic overlay information provided by tracking and instrument generated susceptibility in repeated fast-images as reference. The stylet was removed and the drill was introduced into the trochar. The drill was then advanced to the lesion (Figure 7) and a sample was collected.

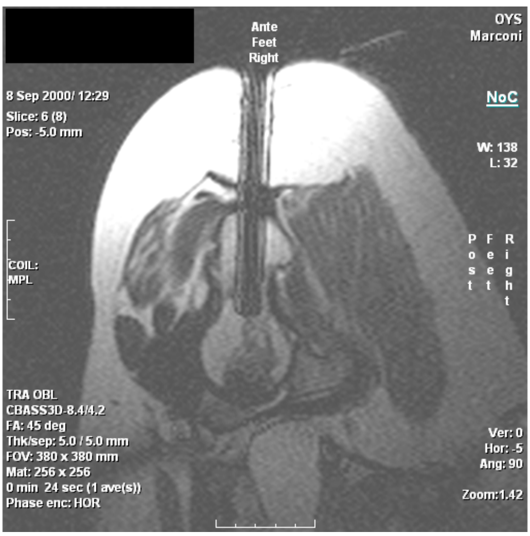

Fig. 7. A biopsy drill in the lesion situated at the femoral head. CBASS, 8 slices, TR 8.4 ms, TE 4.2 ms, slice thickness/interval 5.0 mm/5.0 mm, FOV 380x380, matrix 256x256, acquisition time 24 seconds.

If the catch seemed insufficient to the interventionist, the procedure was repeated through the trochar. The cytologic samples were aspirated through the trochar from the drill channel after the initial trephine biopsy. Before and during the puncture, fast T1-weighted gradient (3 slices, FE, TR 95 ms, TE 7 ms, slice thickness/interval 7.0 mm/7.0 mm, FOV 380x380, matrix 300x300, acquisition time 12 seconds), (5 slices, FE, TR 130 ms, TE 11 ms, slice thickness/interval 10,0 mm/10.0 mm, FOV 380x380, matrix 256x256, acquisition time 18 seconds), or CBASS imaging (8 slices, CBASS, TR 8.4 ms, TE 4.2 ms, slice thickness/interval 5.0 mm/5.0 mm, FOV 380x380, matrix 256x256, acquisition time 24 seconds), (1 slice, CBASS, TR 9.1 ms, TE 4.5 ms, slice thickness/ interval 10.0 mm/ 10.0 mm, FOV 380x380, matrix 256x256 acquisition time 1.5 seconds) was performed in order to visualize the biopsy set.

If the immediate preoperative MRI visualization of the lesion was not adequate or preoperative imaging suggested that using contrast agent might be beneficial in visualizing the most active part of lesion, intravenous contrast medium (15 cc of gadolinium) was introduced directly prior to the puncture. Contrast was used in 5 lesions graded edematous, one graded destructive and in one graded sclerotic. T1-weighted fast spin echo imaging (5 slices, FSE, TE 400 ms, TR 16 ms, slice thickness/interval 7,0 mm/ 8.0 mm, FOV 380x380, matrix 324x324, acquisition time 23 seconds) of the lesion was then performed. The patients remained in hospital for 24 hours for routine follow-up.

The trephine biopsy samples were fixed in 10% formalin. The FNA material was processed by fixing the sample in 50% alcohol for preparation by the filtration technique. The FNA findings were rated as cytologic samples: C0 -insufficient; C1 -normal; C2 -benign atypia; C3 -possibly malignant; C4 was highly suspicious of malignancy and C5 was malignant. Grades C3, C4 and C5 were determined to concur with malignant histology. A pathologist determined the amount of obtained trephine biopsy material and FNA material as either sufficient or insufficient for diagnostic use. Histopathological and cytological diagnosis based on trephine biopsy material and FNA material was determined by pathologists. Double reading of the samples was used. After initial histopathological and cytological diagnosis, the samples were re-evaluated by a pathologist experienced in bone pathology. Possible change in diagnosis after this re-evaluation was recorded. The diagnostic accuracy for histology, FNA and bacterial stains was reported as true-positive or true-negative and false-positive or false-negative. Cases determined as being false negative were divided into two groups after 6 months' clinical follow-up: wrong diagnosis or sampling error. Insufficient sample in FNA and necrosis as a diagnosis in trephine biopsy were determined as a non-diagnostic being false negative, and a new biopsy (MR-guided or surgical) was scheduled. The evaluation of diagnostic accuracy was achieved by comparing the histopathological diagnosis, cytological diagnosis and microbiological diagnosis with current or final diagnosis made during 6 months' clinical follow-up.

4.4 MR-guided periradicular therapy

Patients referred for percutaneous periradicular nerve root infiltration therapy at our institution during April 1 1999-March 1 2001 were included in the study. The series consisted of 61 patients, who underwent altogether 67 percutaneous periradicular nerve root infiltrations. The periradicular nerve root infiltration was always targeted to the symptomatic side of the patient. 58 infiltrations were targeted to first sacral root, 7 infiltrations to 5th lumbosacral root and 2 to 4th lumbosacral root. On 5 patients double infiltration was performed from 4 to 10 months after to the first procedure due to renewed radicular pain. One patient had periradicular nerve root infiltration also to the contra-lateral nerve root. The mean age of the patients was 46 years (range 22-71 years); 41 patients had an unoperated disc disease and 20 patients had history of previous back surgery. All patients had lumbosacral radicular pain or sciatica diagnosis set by surgeon or rehabilitation specialist before referral to the procedure. Patients with indication for acute surgery, such as cauda equina, were excluded from the study. The final outcome of procedural pain relief obtained was evaluated after 6 months' clinical follow-up and questionnaire. The effect to the radicular pain was graded:

1. Good to excellent = no pain or not disturbing pain allowing normal physical activity at 3 months from the procedure,
2. Temporary = temporary relief of pain (1-4 weeks),
3. No relief of pain
4. Worsening of pain.

All the patients had a preprocedural MRI or CT study made.

The possible correlation between the effect of nerve root infiltration therapy and the etiology of the pain was studied. To facilitate this the findings of vertebral disc anatomy and pathology causing possible narrowing in subsequent path of the symptomatic nerve root in individual patients were classified into 3 categories at the lumbosacral levels from L1 to S1. This classification was done by inspecting the pre-procedural imaging data (MRI or CT) obtained from the lumbosacral area.

The categories were;

1. Normal or minor protrusion of intervertebral disc without narrowing of the nerve root space.
2. Intervertebral disc herniation narrowing the nerve root space.
3. Narrowing of the nerve root channel due post-operational scarring and/or osseal prominence.

An MRI compatible 20 gauge needle (MReye, Cook, Bloomington, IN, USA or Manan, MD Tech, Fl, USA) was used for nerve root infiltration puncture and injection of therapeutic substance.

A prerequisite for the procedure was a free route to the periradicular nerve root area. The route was determined with T1-weighted fast spin echo imaging (5 slices, FSE, TE 400 ms, TR 16 ms, slice thickness/ interval 7,0 mm/ 8.0 mm, FOV 380x380, matrix 324x324, acquisition time 23 seconds), CBASS (completely balanced steady state) imaging (8 slices, CBASS, TR 8.4 ms, TE 4.2 ms, slice thickness/interval 5.0 mm/5.0 mm, FOV 380x380, matrix 256x256, acquisition time 24 seconds), and T2-weighted fast spin echo images (9 slices, FSE, TE 3500 ms, TR 150 ms, slice thickness/interval 7.0 mm/8.0 mm, FOV 380x380, matrix 192x192, acquisition time 35 seconds), were also obtained whenever no previous MRI imaging had been made. The used sequence, CBASS (completely balanced steady state) is in essence true-FISP type sequence combining T2 and T1 expression based on the T2/T1 balance in using high flip angles. This sequence is fast and allows high resolution compared to other fast imaging sequences used in low-field interventional MRI (Duerk *et al*. 1998).

The nerve root determined preoperatively as being the most probable pain source by clinical inspection and imaging studies was selected as target.

The set-up for therapeutic MR-guided injection and the surface coil used are demonstrated in Figure 2.

To reduce procedural subcutaneous pain, the local anesthetic lidocaine (10%), maximum 5ml, was then injected into the subcutaneous soft tissue. No other medication, sedation or monitoring was used. The needle was then advanced through the subcutaneous fat and dorsal sacrolumbar ligaments to the connective tissue surrounding the nerve root, i.e. periradicular space, using graphic overlay information provided by tracking and instrument generated susceptibility in repeated fast-images as reference, (Figure 8A). The mandrel was removed and 2 ml of saline was introduced into the periradicular space (Figure 8B). This technique was used in the last 62 infiltrations. The possible pain provocation generated and the nature of it were recorded simultaneously.

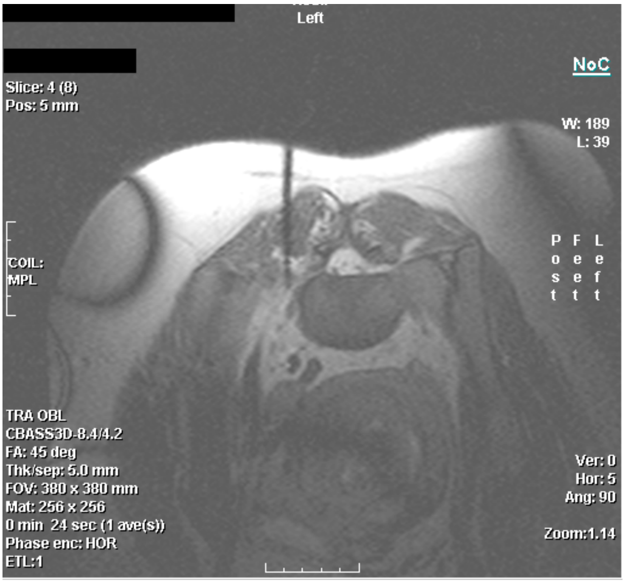

Fig. 8. A Needle at periradicular space of the S1 nerve. 8 slices, CBASS, TR 8.4 ms, TE 4.2 ms, slice thickness/interval 5.0 mm/5.0 mm, FOV 380x380, matrix 256x256, acquisition time 24 seconds.

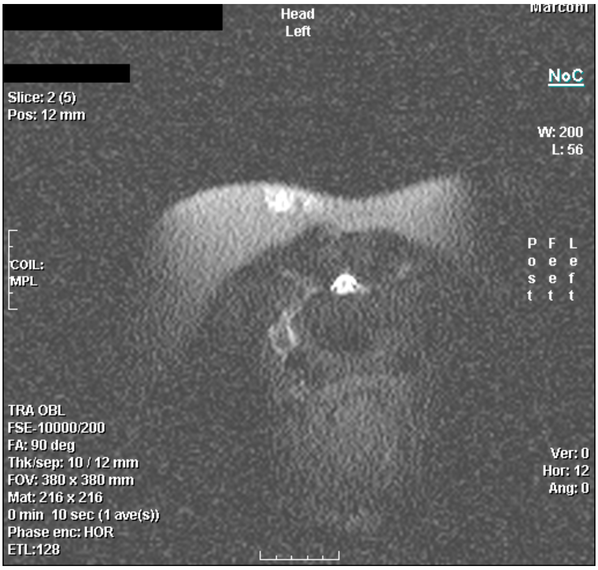

Fig. 8. B Saline is visualized at periradicular space. 5 slices, EXPRESS, TR 9000 ms, TE 274 ms, slice thickness/interval 7mm/7mm, FOV 380x380, matrix 256x256, acquisition time 9 seconds.

Before and during the puncture, fast T1-weighted gradient echo (3 slices, FE, TR 95 ms, TE 7 ms, slice thickness/interval 7.0 mm/7.0 mm, FOV 380x380, matrix 300x300, acquisition time 12 seconds), (5 slices, FE, TR 130 ms, TE 11 ms, slice thickness/interval 10,0 mm/10.0 mm, FOV 380x380, matrix 256x256, acquisition time 18 seconds), or CBASS imaging (8 slices, CBASS, TR 8.4 ms, TE 4.2 ms, slice thickness/interval 5.0 mm/5.0 mm, FOV 380x380, matrix 256x256, acquisition time 24 seconds), (1 slice, CBASS, TR 9.1 ms, TE 4.5 ms, slice thickness/interval 10.0 mm/10.0 mm, FOV 380x380, matrix 256x256 acquisition time 1.5 seconds) was performed in order to visualize the needle and anatomic structures to enable correct needle positioning to the target.

Immediately before and after the introduction of saline to the periradicular nerve root space, a single shot fast spin echo (SSFSE) imaging (5 slices, EXPRESS, TR 9000 ms, TE 274 ms, slice thickness/ interval 7mm/7mm, FOV 380x380, matrix 256x256, acquisition time 9 seconds) was performed to detect fluid signal around or parallel to the nerve root. The final proof of correct placement of the needle was obtained with this method. Possible pain provocation by the injection of saline was also used as an adjunct confirmation of the right placement of the needle.

After this the therapeutic agent was introduced through the needle, either 2 ml of methylprednisolone-bupivacaine solution (Solomet, methylprednisolone 40 mg/ml-bupivacaine 5 mg/ml; Orion, Finland) (63 infiltrations) or 2ml bupivacaine (5%), (4 infiltrations) was injected into the periradicular space and the fluid signal around or parallel to the nerve root was again detected with the SSFSE sequence. In the first 8 procedures fluoroscopy was used with MRI as an adjunct modality either for determining the puncture site to the skin or to confirm the final placement of the needle in the connective tissue surrounding the nerve sheath with a contrast agent.

4.5 MR-guided discography

Between April 1 2000 and March 1 2001 patients referred for percutaneous discography at our institution were included in the study. The series consisted of 12 patients, 6 males and 6 females, mean age being 41 years. Altogether 35 disc punctures were initialized and 34 percutaneous discograms were obtained. All patients had clinical suspicion of lumbar discogenic pain and/or a suggestive finding of lumbar disc or lumbar spine degeneration in imaging studies (MRI, CT, x-ray). Pre-procedural degenerative spine findings and clinical diagnosis of possible lumbar instability verified in lumbar region extension-flexion x-ray images was reported. MR-guided discography was performed in order to determine possible pain provocation during contrast injection as a preliminary test to evaluate the possibility of surgical spinal fusion as a treatment option for continuous pain. The discography was always performed from the less symptomatic side. Patients with indication for acute surgery, such as cauda equina, were excluded from the study. Also excluded were patients with suggestive imaging findings of acute disc herniation, neoplasm, spinal stenosis and infection. All the patients received pre-procedural intra-venous antibiotics, 1.5 g cefuroxime.

The final incidence of possible procedural complications was evaluated after 6 months' clinical follow-up. The primary result of possible surgical operation was evaluated 6 months after surgery. 9 patients underwent MRI study of the lower back area immediately before the MR-guided discography. The MRI study with same sequential configuration was repeated immediately after the MR-guided discography for these 9 patients. The diagnostic MRI study used consisted of non-contrast sagittal FSE T1 (13 slices, FSE, TE 380 ms, TR 18 ms, slice thickness/interval 5.0 mm/5.5 mm, FOV 320x320, matrix 256x256, acquisition time 5 min 46 seconds), FSE T2 (13 slices, FSE, TE 4500 ms, TR 120 ms, slice thickness/interval 5.0 mm/5.5 mm, FOV 320x320, matrix 256x256, acquisition time 7 min 12 seconds). In addition, axial 3D T1 gradient echo imaging (24 slices, FE3D, TE 33 ms, TR 9 ms, slice thickness/interval 3.0 mm/3.0 mm, FOV 350x350, matrix 256x256, acquisition time 7 min 36 seconds) was performed preoperatively and after injection of contrast media to obtain MRI discograms.

A prerequisite for the procedure was a free route to the lumbar disc area. The route was determined with T1-weighted fast spin echo imaging (5 slices, FSE, TE 400 ms, TR 16 ms, slice thickness/interval 7.0 mm/8.0 mm, FOV 380x380, matrix 324x324, acquisition time 23 seconds) and CBASS imaging (8 slices, CBASS, TR 8.4 ms, TE 4.2 ms, slice thickness/ interval 5.0 mm/5.0 mm, FOV 380x380, matrix 256x256, acquisition time 24 seconds).

The typical patient set-up for MR-guided discography is demonstrated in Figure 2.

To reduce procedural subcutaneous pain the local anesthetic lidocaine (5ml) was then injected into the subcutaneous soft tissue. No other medication, sedation or monitoring was used.

Before and during the puncture, a T1-weighted gradient echo (3 slices, FE, TR 95 ms, TE 7 ms, slice thickness/interval 7.0 mm/7.0 mm, FOV 380x380, matrix 300x300, acquisition time 12 seconds), (5 slices, FE, TR 95 ms, TE 7 ms, slice thickness/interval 7,0 mm/7.0 mm, FOV 380x380, matrix 256x256, acquisition time 18 seconds), or CBASS imaging (8 slices, CBASS, TR 8.4 ms, TE 4.2 ms, slice thickness/interval 5.0 mm/5.0 mm, FOV 380x380, matrix 256x256, acquisition time 24 seconds), (1 slice, CBASS, TR 9.1 ms, TE 4.5 ms, slice thickness/interval 10.0 mm/ 10.0 mm, FOV 380x380, matrix 256x256 acquisition time 1.5 seconds) was performed in order to visualize the needle.

The initial puncture was performed with an MRI compatible 19.5 gauge needle (Chiba-type MReye™, Cook, Bloomington, IN, USA). This needle was used as a coaxial needle. The needle was then advanced through the subcutaneous fat and dorsal sacrolumbar ligaments and muscles to the edge of the intervertebral disc using both the graphic overlay information and the instrument generated susceptibility artifact in repeated fast-images as reference. The inner mandrine was then removed and initial disc puncture was performed through the co-axial needle with 22 gauge needle (Manan-type, MD Tech, Fl, USA), which was advanced to the centre of the intervertebral disc; Figures 9 and 10.

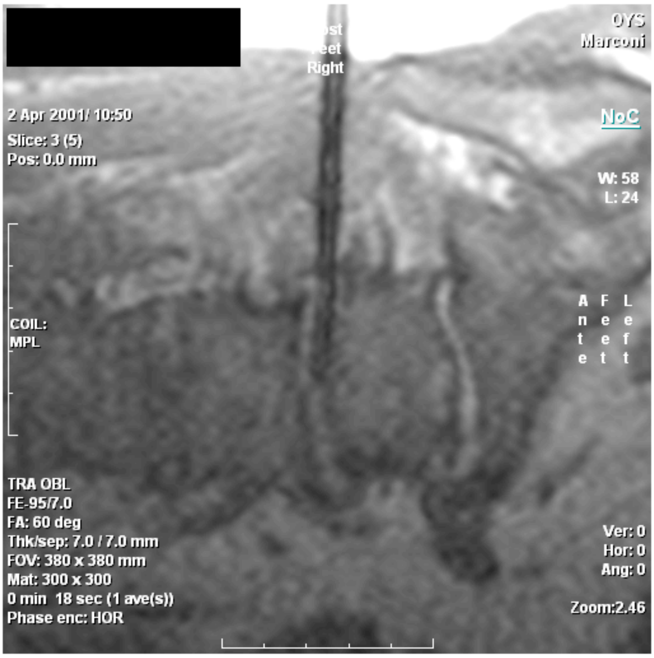

Fig. 9. A sagittal image of the needle in the intervertebral disc. 5 slices, FE, TR 95 ms, TE 7 ms, slice thickness/interval 7.0 mm/7.0 mm.

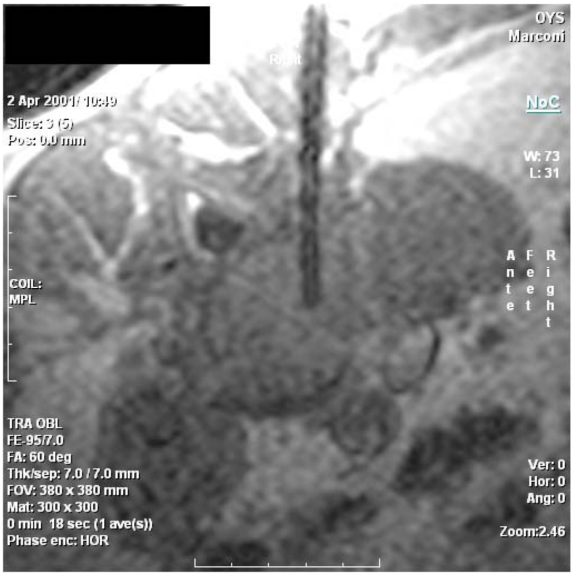

Fig. 10. An axial image of the needle in the paravertebral disc. 5 slices, FE, TR 95 ms, TE 7 ms, slice thickness/interval 7.0 mm/7.0 mm.

After disc puncture 1-2ml of gadolinium-saline mixture (1:8) was injected into the disc. The possible pain provocation generated and the nature of it were recorded simultaneously. Immediately after injection sagittal FE T1 weighted images were obtained to verify the formation of MRI discogram (Figure 11).

Fig. 11. Sagittal FE T1 weighted discogram image. 5 slices, FE, TR 95 ms, TE 7 ms, slice thickness/interval 7.0 mm/7.0 mm.

Evaluation of the pain patient experienced was done during injection of contrast by evaluating pain concordance with patients' existing pain symptoms using the Dallas Discogram Description scale (Sachs *et al*. 1987) for injection-generated pain: no sensation, pressure, dissimilar pain, similar pain, exact pain reproduction. For this study pain reproduction was classified as concordant when the patient felt similar or exact reproduction of pain. Non-concordant pain reproduction was reported when the patient felt the sensation of dissimilar pain, pressure or no pain during injection of contrast.

4.6 MR-guided laser induced thermotherapy of osteiod osteoma

Between September 1 2001 and May 1 2002 5 consecutive patients (mean age 26 years, 3 females, 2 males) with clinical and imaging findings suggesting osteoid osteoma were treated with interstitial laser treatment at our department.

The patients' lesion localization sites were; femur (n=4), talus (n=1), mean nidus size was 1.3 cm. Lesion sizes and localizations are demonstrated in Table 4.

Table 4. Osteoid osteoma patients' age, lesion size, localization, diagnosis and outcome.

Patient	Size	Localization	Diagnosis	Outcome
16 y	2cm	Femur	Ost.osteoma	Residivation,5 months
11 y	0.5cm	Talus	Ost.osteoma	Complete recovery
61 y	2cm	Femur	Fibrosis	Complete recovery
17 y	1cm	Femur	Fibrosis	Complete recovery
24 y	1cm	Femur	Ost.osteoma	Complete recovery

Strict sterility was maintained throughout the procedure. All the patients received prophylactic antibiotics before procedure, cefuroxime 1,5 g iv.

Depending from the patients age, lesion localization and patient co-operation either general anesthesia or spinal anesthesia was used. If general anesthesia was used local anesthetics were applied (lidocain 5%) subcutaneously to the treatment area to ease post-procedural local pain.

Initial puncture to the lesion was done under MR-guidance using the described optical instrument guidance. The needle was then advanced through the subcutaneous fat to the target vicinity using graphic overlay information provided by tracking and instrument generated susceptibility in repeated fast-images as reference. Before and during the puncture CBASS imaging (8 slices, CBASS, TR 8.4 ms, TE 4.2 ms, slice thickness/ interval 5.0 mm/5.0 mm, FOV 380x380, matrix 256x256, acquisition time 24 seconds), (1 slice, CBASS, TR 9.1 ms, TE 4.5 ms, slice thickness/interval 10.0 mm/10.0 mm, FOV 380x380, matrix 256x256 acquisition time 1.5 seconds) and FE imaging (5 slices, FE, TR 95 ms, TE 7 ms, slice thickness/interval 7.0 mm/7.0 mm, acquisition time 18 seconds) was performed in order to visualize the instrument and anatomic structures to enable correct instrument positioning to the target.

A 14 g bone biopsy drill (Cook Medical, USA) (Figure 12) was used to enter nidus (Figures 13 and 14).

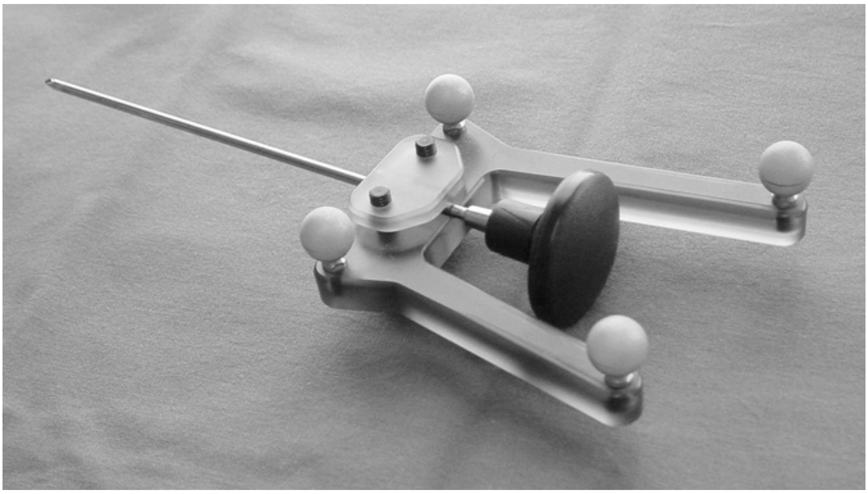

Fig. 12. A 14 g bone biopsy drill with optical tracking instrument holder.

Fig. 13. Bone biopsy drill adjacent to osteoid nidus. 5 slices, FE, TR 95 ms, TE 7 ms, slice thickness/interval 7.0 mm/7.0 mm, acquisition time 18 seconds.

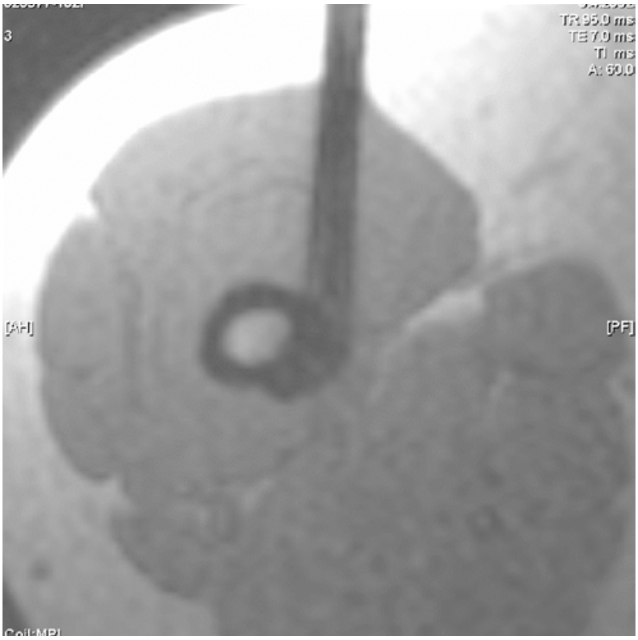

Fig. 14. Bone biopsy drill in the osteoid nidus. 5 slices, FE, TR 95 ms, TE 7 ms, slice thickness/ interval 7.0 mm/ 7.0 mm, acquisition time 18 seconds.

A subsequent biopsy was extracted. After drilling the channel to the lesion nidus a 14 g coaxial needle (MRI devices Daum, USA, Germany) was introduced to the channel via MRI compatible 0.35 stiff guidewire (Somatex GmbH, Berlin, Germany) and its position was controlled with imaging. The guidewire was then removed and laser fiber was introduced to the needle shaft. The needle was then retracted 0.5 to 1 cm and its position was again controlled. After this the laser treatment was initialized.

The used laser device was of Nd-Yag type, maximum power 100W (Fibertom medilas, Dornier Medizin technik, Germany). A bare laser fiber (Dornier Medizin technik, Germany) with a 400 µm diameter of was used. The laser treatment was conducted using constant energy flow and power of 2 W. The mean amount of energy delivered to the bone tissue was 1,000 joules (min 350 J, max 1,800 J). The maximum energy amount not to be exceeded was calculated from the formula derived from the results of earlier studies, where the increase of bone tissue coagulation size was measured with increase of laser induced energy deposition (Gangi *et al.* 1997c). Least square fit was introduced to this data and a logaritmic correlation (R^2 between 0.93 and 0.99) was found between the laser energy and coagulation size, both in the axial and longitudial direction. This was true in both groups in earlier study. That study showed also that increasing the laser energy increases the coagulation size only to a certain value, between 6mm and 10 mm, after which increase in the laser power yields very little increase in the coagulation size. The formula acquired with square fit for axial coagulation is

$$D = 2{,}389*\ln(E)-10{,}58,$$

where D is the coagulation diameter in millimeters and E the laser energy. The treatment was monitored by using CBASS MRI imaging, (CBASS 3D, TE 7.7 ms, TR 3.8 ms, 8 slices, slice thickness/interval 6.0 mm/6.0 mm, FOV 380x380, matrix 160x160, FA 63 deg., acquisition time 24 seconds), by following the change in signal intensity expressed as signal void in the image caused by the temperature change in the tissue heated. Imaging sequence was repeated at 1minute 30 seconds intervals. When possible signal void was detected and maximum amount of energy delivered the treatment was considered complete. After the treatment the patients were monitored for 6 hours in the recovery room. The patients were dispatched from the hospital after the first clinical control performed within 24 hours of the treatment. A further clinical control was carried out within 3 weeks after the procedure. A questionnaire for each patient on the status of pain symptoms was filled in by the patients 3 and 6 months after the treatment. The questionnaire was structured as 1. total relief of pain 2. some relief pain 3. no relief of pain. Only total relief of pain was considered as successful outcome. In case of persisting pain patients were rescheduled for control MRI study and re-treatment with laser ablation.

5 Results

5.1 Guidance method for MR-guided bone biopsy

The bone biopsy system was successfully applied to all patients, and it provided a safe and accurate guidance method for all phases of the procedure. Optical tracking implemented as part of the biopsy set allowed the puncture route to be chosen fast and reliably before needle insertion, and it was also useful during the biopsy procedure whenever the angle of approach had to be changed. Optical tracking also allowed almost real-time imaging in the plane of the instrument, which made the procedure easy to accomplish in different anatomical areas and at different angles of approach, allowing the procedural time from the insertion of the needle through skin to needle retraction to be less than 40 minutes.

The biopsies performed using this system yielded sufficient samples in all cases (Table 2). One of the vertebral body biopsies (Th 7) was performed via the transpedicular route without difficulties (Figure 15).

Fig. 15. Transpedicular vertebral biopsy. Sagittal image. CBASS, 8 slices, TR 8.4 ms, TE 4.2 ms, slice thickness/interval 5.0 mm/5.0 mm, FOV 380x380, matrix 256x256, acquisition time 24 seconds.

The image quality of the 0.23 T scanner was sufficient in all cases, including lesions diagnosed with high-field MRI prior to the intervention. No complications occurred.

5.2 MR-guided bone biopsy

The low-field MRI device used detected all the lesions in the patients referred for biopsy. The lesions were seen both in the immediate preprocedural scans using conventional sequences and in the fast imaging sequence scanning used during the procedure. In all but one case, the location of the lesions was such that a safe approach was possible using MR-guidance, and the needle could also be detected in all lesions. In one patient, a conversion to CT guidance was made. A motion artefact due to inadequate procedural imaging quality caused this; the lesion was situated at the thoracic vertebral body and at the time of procedure fast scanning sequence (CBASS), which is less sensitive to motion, was not available. MR contrast medium was used in 7 out of the 13 MRI biopsies performed in order to improve visualization of the active component of the lesion. However, no improvement in visualization of the lesion was found in cases when contrast was used.

Out of the 13 patients biopsied in MRI, the trephine biopsy yielded a diagnosis in all but one case. All the double and triple samples concurred. Double reading of sample material did not result in changes in initial diagnosis. One of the trephine biopsy findings was considered false negative during 6 months' clinical follow up. This was categorized as a sampling error and the final diagnosis was achieved with surgical biopsy. Diagnostic accuracy in the trephine biopsy series was thus 95%. The trephine biopsy yielded a malignant diagnosis in 4 patients, a post-infectious or granulomatous reaction in 4 patients, a benign fibrotic lesion in 2 patients and Paget´s disease in one patient, while two patients had a normal finding after a 6-month clinical follow-up. MRI guided trephine biopsy excluded malignancy in 3 patients with a known previous malignant disease and detected malignancy in 3 patients without a previous diagnosis of malignant disease.

The FNA sample material was adequate for diagnostic evaluation in all cases. The FNA cytological diagnosis concurred with the trephine biopsy diagnosis in 54% of cases. There were thus 46% of false negatives in FNA diagnoses, which were all determined to be due to sampling error. However, the cytological diagnosis concurred with histological diagnosis in all cases with malignant histology. The bacterial stains for microbiological diagnostics were true negative in all of the 4 cases where they were collected with a 6-month clinical follow-up.

The mean puncture time from the introduction of the needle through skin to needle retraction was 1 hour 20 minutes. The mean operative time from entering the interventional MRI operation theater to leaving it was 2 hours 55 minutes, maximum 4 hours 30 minutes and minimum 1 hour 45 minutes, this included the anesthesia procedures needed. The mean number of sequences used during the procedure was 26, maximum 58 and minimum 8 sequences. There were no procedural complications.

5.3 MR-guided periradicular therapy

All the nerve roots selected for targeted infiltration were detected in the low-field MRI device used. MR-guidance allowed correct needle positioning in all but one case (98.5%) when MR-guidance was used. The failure was caused by degeneration-induced changes in anatomy obstructing path to the nerve root canal. There was no need to reposition the needle after initial MRI imaging (8 slices, CBASS, TR 8.4 ms, TE 4.2 ms, slice thickness/interval 5.0 mm/5.0 mm, FOV 380x380, matrix 256x256, acquisition time 24 seconds) had confirmed the localization of the needle in the direct vicinity of the nerve root sheath.

The mean puncture time from the introduction of the needle through skin to needle retraction was 12 minutes, minimum 2 minutes and maximum 60 minutes. The mean procedural time from starting the interventional MRI procedure to completing it was 33 minutes, minimum 9 minutes and maximum 84 minutes, this included the anesthesia procedures needed. These times do not include the time required for preparing the patient and operation room. The mean total number of sequences used in all scans during the procedure was 13, minimum 7 sequences and maximum 26. The mean number of sequences used for puncturing was 10, minimum 2 and maximum 20. There was one case where post-procedural pain was categorized as a post-procedural complication. Three patients underwent back surgery during follow-up period due to persisting clinical symptoms and worsened disc pathology finding in imaging studies. All these patients had relief to the pain from surgery.

The therapy effect outcome of all performed punctures is shown in Table 5.

Table 5. The effect of nerve root infiltration to the radicular pain in all performed punctures.

The effect of nerve root infiltration on radicular pain	N	%
No pain or not disturbing pain	35	52.2
Temporary relief of pain	15	22.4
No relief of pain	14	20.9
Worsening of pain	3	4.5
Total	67	100.0

For these data statistical analysis was performed with a chi-square test where $p < 0.001$, $df = 3$, and $\chi^2 = 31.806$.

Effect of nerve root infiltration on the radicular pain according to the operational situation before the procedure is shown in Table 6.

Table 6. Effect of nerve root infiltration on radicular pain according to the operational situation before the procedure.

The effect of nerve root infiltration on radicular pain	Patients' operational situation before nerve root infiltration			
	Operated		Not operated	
	N	%	n	%
No pain or not disturbing pain	15	78.9	18	41.9
Temporary relief of pain	2	10.5	11	25.6
No relief of pain	2	10.5	11	25.6
Worsening of pain	-	0.0	3	7.0
Total	19	100.0	43	100.0

The therapy effect on patients with different types of nerve root channel narrowing is shown in Table 7.

Table 7. The therapy effect on patients with different types of nerve root channel narrowing.

The effect of nerve root infiltration to the radicular pain	Type of finding in preprocedural imaging					
	A disc herniation finding		Narrowing of the nerve root channel findings due to post-operational scarring and/or osseal prominence		Normal or symmetrically protruded disc without narrowing of the nerve root channel findings	
	n	%	5	%	n	%
No pain or not disturbing pain	23	62.2	2	18.2	3	25.0
Temporary relief of pain	8	21.6	6	54.5	1	8.3
No relief of pain	4	10.8	3	27.3	7	58.3
Worsening of pain	2	5.7	-	0.0	1	8.3
Total	37	100.0	11	100.0	12	100.0

Of all infiltrations, 63 were done with methylprednisolone-bupivacaine solution, the outcome being good to excellent in (n=33) 52.4%, temporary relief in (n=15) 23.8%, (n=12) 19% had no effect, and (3) 4.8% had worsening of pain. With the four infiltrations done with bupivacaine alone, (n=2) 50% patients had good or excellent outcome and (2) 50% patients had no effect.

Saline solution served as the contrast agent for heavily T2-weighted SSFSE imaging sequences in the last 62 infiltrations. In all of these the contrast to noise ratio was sufficient to confirm the right placement of the needle and allowed visualization of the path of the nerve root treated.

5.4 MR-guided discography

A total of 35 discs were punctured and 34 procedural MRI-discograms were obtained on 12 patients. This yielded the procedural success rate of 97%. The anatomic distribution of punctured disks was following: 3 (9%) discs at the L2-to L3 level, 12 (35%) discs at the L3-to L4 level, 12 (35%) discs at the L4-to- L5 level and 7 (21%) discs at the L5- to S1 level. In all injections a positive or negative pain response from targeted discs was obtained, generating 100% success in assessing pain response.

The average time for performing MR-guided discography was 1 hour 25 minutes (min. 45 minutes, max. 2 hours 15 minutes) for 3 discs and the average number of imaging sequences used for puncturing one disc was 12. Average time to perform MR-guided discography on one disc was 19 minutes (min. 5 minutes, max. 50 minutes). There was one complication reported (disc collapse) during follow-up. In one disc the puncture failed and discogram was not acquired. Post-procedural axial MRI-discogram was acquired from 9 patients (Figure 16), making up a total of 25 discs.

Fig. 16. An axial discogram image. 24 slices, FE3D, TE 33 ms, TR 9 ms, slice thickness/interval 3.0 mm/3.0 mm, FOV 350x350, matrix 256x256, acquisition time 7 min 36 seconds.

5.5 MR-guided laser induced thermotherapy of osteiod osteoma

The mean operative time from starting the procedure (image localization) to the end of the procedure (retracting the laser fiber) was 95 minutes. The mean amount of interventional imaging sequences used during the puncture was 11.

All the 5 treatments were successful. A definite proof signal change in MRI images of the treatment area taken during thermal treatment was not observed. All the patients were discharged from hospital within 48 hours from the procedure. All the patients were symptom-free 3 weeks after the initial laser treatment. There were no complications during follow-up time (6 months). Biopsy resulted in diagnosis of osteoid osteoma in 3 cases (75%) and fibrosis in 2 patients (25%). There was one recurrent osteoid ostema during follow-up.

6 Discussion

6.1 Low field imaging & integrated optical instrument tracking

Open configuration MRI scanners possess several attributes that make them favorable as an interventional system compared to other imaging modalities or closed high-field MRI systems. High field scanners put far greater demands on patient safety due to high B0. Patient access is also a problem.

An open configuration MRI device allows good access to the patient. Furthermore, there is seldom any need to move the patient during the operation. A low field scanner can typically be easily and quickly shut down facilitating fast conversion in procedures if needed. Supplementary and accessory technical hardware is easier to protect and use in low- or mid-field surroundings. These facts are bound to affect patient safety.

When compared to conventional imaging modalities MR-guidance allows the freedom to choose any imaging plane. This facilitates the technical task of performing interventional procedures at oblique angles. The optical tracking facilitates real-time control of instrument position in relation to the image data and is easy to use. Combined with the operator controlled sequence start with foot pedal and fast imaging the system increases operator control, thus increasing the speed and accuracy of the procedure. The advantage of this was also shown in our studies, where high technical accuracy was achieved almost without complications. The disadvantages of optical tracking are the trackers' need of line-of-sight and relative insensitivity to needle bending.

The most critical phase of performing minimally invasive procedures is the accurate and safe positioning of the needle. Dissimilar needle artifact sizes in different sequences under MR-guidance must be taken in account for (Butts *et al*. 1999). In general, needle artifact in MRI image is much more prominent in gradient echo images than in T1 weighted FSE and T2 weighted FSE images. The needle thickness also affects artifact size; the removal of mandrel diminishes the artifact size in MRI image. The needle position in relation to the main magnetic field (B0) also has considerable effect. A more perpendicular needle position with respect to B0 orientation produces more pronounced needle artifact. The needle path should be planned accordingly.

Needle bending due to needle material (titanium-alloys) must be taken into account, as the correct position should be unambiguously ascertained. In practice this means confirmatory images where the needle artifact or injected contrast agent are clearly visible. In MR-guided nerve root infiltration needle bending can be easily controlled by thicker slice set if necessary.

With MR-guidance there is no irradiation burden on the patient or the physician, which is advantageous in performing procedures on adolescents and potentially pregnant females but particularly important for physicians when considering the interventional radiologist's radiation burden general. It is also generally acknowledged that interventional procedures should be performed without ionizing radiation whenever feasible. The European Union also has established guidelines advocating the use of MRI instead of modalities with ionizing radiation involved when the expected level of information or therapeutic result is equal (European Commission 2001, and European Union 1997).

Still, MRI interventions are not as easily conducted as fluoroscopic interventions. In terms of imaging speed, MRI is comparable to conventional CT but not to CT fluoroscopy. The slower imaging speed in MRI is not a problem if real-time optical tracking is available. CT has superior axial resolution, and the ability to detect pneumothorax favors the use of CT in the thoracic region. However, in all of our series it was found that image quality of operative images obtained with a 0.23 T scanner was sufficient to guarantee a safe procedure.

The superiority of MRI as a guidance modality is evident due to its good sensitivity, good visualization of the lesion and accuracy. The potential and actual excellent clinical results have established MRI as a guidance modality comparable to the others in performing interventions.

MR-guidance is used successfully in many indications where the use of MRI has the potential of yielding supplementary information on the target and its surroundings. MRI has already emerged as a reliable tool for numerous interventional procedures (Adam *et al*. 1999, de Jode *et al*. 1999, Law & Regan 2000, Fiedler *et al*. 2001, Koenig *et al*. 2001, Vogl *et al*. 2001).

MR-guidance in interventions has several advantages when compared to traditional modalities. MRI is able to detect lesions not seen at all in other modalities. MRI also has superior soft tissue resolution, with or without contrast, even in interventional sequences. Also bone interventions can be reliably conducted (Koenig *et al*. 2001).

Despite all the inherent advantages of MRI in interventional use there are also some challenges that must be met. All MR-guided interventions require special safety demands to be fulfilled in order to ensure a safe procedure. All the equipment within the imaging area must be MRI-safe, naturally including all the instrumentation. Instrument safety is one of the key issues in IMRI. At the moment, MRI-compatible instrumentation is relatively highly priced and not so easy to come by. Although most of the major instrument manufacturers do have MRI compatible equipment to offer, none seems to have a truly extensive coverage of the instruments needed at the field of IMRI. The initial high cost of the IMRI system is relative a burden, low-field MRI systems are comparable to CT devices in this respect. In can be stated, however, that these facts do not challenge the actual feasibility of MRI interventions. Further assessment of clinical data is however essential to establish cost effectiveness of IMRI procedures.

In this study the difference of modality specific procedural time between different modalities used for interventional procedures was not evaluated. It is to be noted that such studies are warranted.

6.2 Guidance method for MR-guided bone biopsy

Real-time imaging with MRI is often limited by the achievable signal-to-noise ratio and tissue contrast. Therefore, a modality-independent method for localizing the instrument in real time is beneficial on less frequently updated images: an optical tracking system augments this localization by providing instantaneous feedback (Schenck *et al*. 1995, Silverman *et al*. 1995), while intraoperative MRI is used for generating updated roadmaps along the needle path. Compared with passive tracking, where the needle artifact alone is used for deducing the instrument's position and orientation (Lewin *et al*. 1996), optical tracking offers distinct advantages. The initial needle orientation at the puncture site can be determined with the aid of graphic tools and/or needle-guided scout images, whereas passive tracking requires more elaborate slice positioning and MR-visible markers. In this series, determination of the puncture site was possible with optical tracking overlays in one or two MRI sets, and no skin markers were needed. Difficulties in pinpointing the exact orientation of the needle from its artifact have adverse effects on the overall accuracy of needle alignment, and the acquisition of affirmative images accrues a time penalty. Other active guidance systems, such as ultrasound probes and mechanical arms (Barnett *et al*. 1993, Rohling *et al*. 1995) could also be used instead of optical systems, but they lack the flexibility of wireless instrument tracking.

Optical tracking has been successfully used in CT (Jacob *et al*. 2000) and MR-guided needle biopsies and injections (Silverman *et al*. 1995) as well as in surgical operations (Caversaccio *et al*. 1999, Vorbeck *et al*. 2000). Direct attachment of the needle to the optical tracking system was beneficial in deep neural drug injections (Ojala *et al*. 2000). Bending of the needle makes confirmatory imaging more important in fine-needle biopsies and injections than in procedures done with a stiff instrument, such as bone biopsy which was applied in our study. In bone biopsy, optical tracking potentially reduces the need for imaging during the procedure and thus diminishes the procedure time. A wireless solution for optical tracking was even more important in procedures where the instruments are heavy and clumsy, as it helped to avoid the extra disturbance caused by handling the instrument by wires.

The MR-guidance system described here is a comparable method to conventional CT, and although CT-fluoroscopy can provide true real-time imaging its use is limited because of ionizing radiation.

6.3 MR-guided bone biopsy

This study suggests that percutaneous MR-guided bone biopsy is safe and accurate.

Percutaneous or surgical biopsy is the method of choice for diagnosing bony lesions. The most common presentation of a bone lesion is that of a lytic or blastic lesion, and in a patient with a neoplastic history the diagnosis is straightforward. However, if there is no neoplastic history or such history dates back several years, a biopsy is certainly needed. Even if the lesion is presumably metastatic, it is sometimes useful to obtain a biopsy, particularly if there is no previous history of metastatic disease. Correct assessment of information obtainable from lesions of infectious, malignant or benign origin is essential for the selection of effective treatment.

Due to its good sensitivity, MRI is able to detect lesions not seen at all in other modalities. Particularly, lesions with edema, often seen only in MRI as a bright involvement of bone marrow in heavily T2 weighted sequences and STIR sequences can be reliably visualized and readily biopsied (Hoane *et al*. 1991, Kaplan *et al*. 1998, Adam *et al*. 1999). MRI also provides superior tissue contrast without contrast medium. There are also results suggesting that the use of contrast medium may contribute to the accuracy of bone lesion detection in MRI. This is the case especially in recurrent malignancies and in certain types of cartilaginous lesion (Geirnaerdt *et al*. 1998). Contrast media has been used effectively in MRI guided biopsies (Parkkola *et al*. 2001). However, in our study no advantage in lesion visualization was found when contrast was used. It is to be noted that our data did not include any primary malignancy of bone, soft tissue or cartilaginous tumors and this may reflect the poor result of contrast contribution in our study. In taking biopsy from primary bone malignancies it is advisable to use contrast medium, as it is likely to increase the accuracy of biopsy by pointing out the enhancing dimensions of tumor (Parkkola *et al*. 2001). It is also important to know the exact anatomic proportions of the tumor. In primary bone tumors, choosing the proper biopsy route is of utmost importance since removal of the biopsy channel is mandatory during surgery.

CT has superior axial resolution, which favors the use of CT as a guidance modality in bone biopsies. However, in our series all the bone lesions detected preoperatively with CT, high-field MRI or scintigraphy were also seen in operative images obtained with a 0.23 T scanner. Image quality was sufficient in the thoracic region to guarantee a safe procedure. However, we had one conversion to a CT-guided procedure in a patient with thoracic vertebral body lesion. This was before the initialization of fast imaging sequences took place and at that time image quality was considered not sufficient to allow procedure in the thoracic area. After fast imaging sequences were introduced into routine use, no conversions were needed. The spatial resolution capability of MRI remains a controversial issue, at least in the low-field scanners. Unless fast sequences with relatively good resolution, such as CBASS/true-FISP, are used, the procedures targeted to the areas containing fine bony structures should be done under CT-guidance. In the vertebral region the pedicles and cervical area must be considered as such structures.

General anesthesia was used in 6 patients and spinal anesthetics in 8 patients. Although bone biopsies have traditionally been made under local anesthesia, there is a general consensus in the Oulu University Hospital after 15 years of experience in percutaneous bone biopsies that patients do feel more uncomfortable and more pain when using local anesthetics. It is felt that in a patient group where sacro-lumbar and lower extremity region is biopsied, best patient compliance is achieved with spinal anesthetics. General anesthesia is used when performing bone biopsy in children and young patients or patients with lesion in thoracic or head and neck area. Thoracic area biopsy is controversial since optimal visualization in low field is acquired trough minimizing motion-generated artifacts in image. Hence in the thoracic area the breathing motion causes artifact. To minimize this motion during biopsy procedure in thoracic area breath-hold technique can be used. This is however only possible in local anesthesia since spinal anesthesia without ventilation cannot be safely applied when operating at the thoracic area. The next choice is to use generated apnea under general anesthesia during imaging to achieve best image quality. To minimize patient motion and pain and to maximize image quality general anesthesia was used in thoracic area biopsies.

Complete statistical analysis was not made due to small number of patients.

Despite the small number of patients, however, the trephine biopsy results of a success rate of 92% are comparable to the results obtained in CT studies published on this topic. Tikkakoski *et al*. reported diagnostic success rate of 84% in their study which was performed in CT (Tikkakoski *et al*. 1992). Leffler *et al* reported an 82% positive predictive accuracy of CT-guided percutaneous bone biopsy (Leffler & Chew 1999). Ng *et al*. reported an initial success rate of 95% in their study (Ng *et al*. 1998).

In a previous MRI bone biopsy study, sub-optimal sample quality hindered diagnostic efficacy (Neuerburg *et al*. 1998a). This was due to the packing of the sample, which resulted in destruction of the fine structure of the bone. There was no such experience in the series discussed here, and the drill type used seems to provide good-quality samples regardless of the density of the target tissue. There were no procedural complications in this series of MR-guided percutaneous bone biopsies.

FNA has been shown to be informative when taken in conjunction with bone biopsy (Tikkakoski *et al*. 1992). The results of our study are however controversial, with only nominal information advantage gained from performing FNA. The obvious advantage of FNA diagnostics is the relative quickness when compared to bone histology, where the preparation of the sample can take weeks, whereas cytological diagnosis can be obtained within hours. It must be stated, however, that despite the less than optimal overall performance, the cytological diagnosis concurred with histological diagnosis in all cases with malignant histology. This result is probably due to general morphological changes associated with the malignant disease in bone tissue: in malignant disease there is a profound damage in bone structure caused by malignant infiltration, and thus it is easier to obtain cell material in FNA biopsy.

It is concluded that although the number of cases is limited in this study it seems that MR-guided percutaneous bone biopsy is safe, accurate and feasible to perform. It seems also that no significant complications appear to be associated with the procedure. Fine needle biopsy is advantageous when malignant disease is suspected. MRI can be used as the sole modality or with optical tracking guidance in bone biopsies or as a backup modality in performing procedures not possible otherwise. When available, MR-guidance can be favored as a method of choice in performing percutaneous bone biopsies.

6.4 MR-guided periradicular therapy

In this study it was shown that MR-guided nerve root infiltration is safe and accurate. Fluoroscopy or CT-guided procedure is usually the method of choice for nerve root infiltration therapy in the lumbosacral area. Although fluoroscopy is cheap and easy to apply, it does have disadvantages of use in guiding interventions. Firstly, the procedural steering must be done according to bony anatomical landmarks and any variation or change in the soft tissue morphology due to anatomical variation or pathology is not detected. The use of contrast media does little to overcome this dilemma, since when contrast is injected only the edges of adjacent structures to the needle are readily visualized. Secondly, there is radiation burden to the operator and to the patient. Although CT-guidance is far better in identifying anatomical structures at the procedure area, it too has restrictions. Despite excellent temporal and spatial resolution CT is not so good in differentiating various soft tissue structures from each other without special windowing or HU analysis. CT also shares the problem of radiation with fluoroscopy.

As an adjunct to optical tracking and direct visualization of the needle saline solution was used as contrast agent to visualize the nerve root sheath injected. This proved to be a very effective means of confirming the right placement of the needle. Gadolinium compounds with T1-weighted sequences have been used for this purpose (Seibel *et al.* 1997). However, to this date these compounds have not been accepted for intrathecal use and using saline as contrast agent makes it possible to avoid the possible side-effects of intrathecal or epidural gadolinium infiltration.

There was one patient in whom the worsening of the radicular pain was categorized as a minor complication due to the puncture. This was probably caused by nerve root irritation from the puncture or either of the therapeutic substances used.

Low back disorders are extremely prevalent in all societies, and the rate of caused disability, as well as the costs, have increased - independently of disease prevalence - over recent decades (Frymoyer & Cats-Baril 1991). It is obvious that we cannot solve this dilemma with increasing surgical interventions. Minimally invasive interventional procedures are an option to relieve pain and minimize the risk of disability.

To the authors knowledge this is the first study where the usefulness of MR-guidance in lumbar nerve root infiltration is evaluated. In the referred studies (Seibel *et al.* 1997, Uhlenbrock & Arlinghaus 1997, Weiner & Fraser 1997, Viton *et al.* 1998) the outcome of the first sacral root and lumbar root infiltrations have been evaluated in fluoroscopy-, CT- and MR- guidance. Since 1995, over 1,400 nerve root infiltrations have been performed with fluoroscopy guidance at Oulu University Hospital, and in our experience this method allows the needle to be placed only into the dorsal root canal or dorsal root sheath of the lumbosacral nerve roots and the depth is difficult to estimate. MRI overcomes this problem.

In our study the length of the procedural time decreased gradually from 60 minutes reaching a minimum of 2 minutes. This can be seen as a learning curve development in implementing the procedure.

Previous reports concerning the effect of nerve root infiltration therapy on radicular pain have been promising. In a study of CT-guided lumbar nerve root infiltrations (Uhlenbrock & Arlinghaus 1997), 55% of patients were free of symptoms or had had some improvement when evaluated approximately 4 months after the treatment; 30%

reported temporary improvement, and in 15% there was no change compared with the pre-treatment symptoms. In the recent study (Seibel *et al*. 1997) only 15% of the failed back surgery patients got relief to their symptoms after a single CT- or MR-guided nerve root infiltration, and after four treatments 72% of the patients were symptom-free.

In the present study the patients with irritation after failed back surgery had an excellent outcome from nerve root infiltration therapy, with almost 80% of initial pain free result. It has been reported that 75.4% of patients with radicular leg pain had a successful long-term outcome after lumbar transforaminal epidural steroid injection (Lutz *et al*. 1998). 22 of the 28 patients with lumbar disc herniation had considerable and sustained relief from their symptoms in another study (Weiner & Fraser 1997). The outcome was not evaluated separately for lumbar and sacral nerve roots in these studies. In our series the outcome of nerve root infiltration therapy was in accordance with these other studies using fluoroscopy or CT- guidance (Uhlenbrock & Arlinghaus 1997, Weiner & Fraser 1997, Viton *et al*. 1998). A recent published controlled trial is in accordance with these studies as well (Karppinen *et al*. 2001).

In our study the patients with normal to minor disc pathology and the patients with nerve root channel narrowing due to bony or scar involvement did not have such a good outcome from nerve root infiltration therapy. This is probably due to a more passive nature of underlying disease. In these patient groups the feasibility of the procedure remains controversial. It must be stated, however, that percutaneous nerve root infiltration therapy is an almost complication free, patient friendly procedure when compared to surgery, it can very easily be repeated and can be mastered by any radiologist.

On the basis of the present study, MR-guided needle introduction is an accurate procedure and may be used to substitute conventional techniques for nerve root infiltration. This would be especially useful in cases where there are substantial anatomical or structural changes due variation or pathology. It is concluded that MR-guided nerve root infiltration therapy is safe, accurate and feasible to perform. Nerve root infiltration therapy is effective treatment form to control radicular pain and can be used to substitute more invasive procedures in a selected patient group.

6.5 MR-guided discography

Percutaneous discography is a controversial procedure.

Literature lists it used as a clinical tool in at least 8 indications (Tehranzadeh 1998, Anderson & Flanagan 2000, Carragee 2000); Table 8.

Table 8. Discography indications.

List of most frequent indications
1. Negative MRI, CT or myelogram with equivocal findings for disc disease.
2. Positive multiple finding for disc disease in MRI, CT or myelogram. Discogram discerns symptomatic disc.
3. Presence of equivocal MRI, CT, or myelogram
4. Recurrent back pain in post surgical spine, to differentiate recurrent disc versus scar tissue.
5. To assess diagnostics between recurrent disc and pseudoarthrosis in post-surgical fused spine.
6. Preliminary test to spinal fusion to evaluate discs above or below the would-be fusion level.
7. Preliminary test for chemonucleolysis
8. Preliminary test prior to cortisone or anesthetic injection to disc.

Some of these indications have much argued grounds (Carragee 2000). However, the unifying element in all indications of discography is the low back or rather spinal area pain, which is usually conjoined to a situation where other tests or imaging studies findings are not sufficient to allow diagnosis and treatment. It must be noted that the use of discography to assess diagnostics on litigation basis has poor results (Carragee 2000). The most effective use of discography as a diagnostic tool is achieved when it is used for pre-surgical evaluation on patients forwarded for fusion operation (Vamvanij *et al*. 1998, Derby *et al*. 1999, Carragee 2000). All the patients included in this study were forwarded to the discography by orthopedic surgeon in order to determine disc pathology, which would affect possible prognosis and the extent of fusion operation.

In our study we wanted to find out whether MRI guided discography is feasible or not. In this study the technique for diagnostic MRI-guided discography in a low field surroundings is presented. To the author's knowledge this has not been reported before. MRI-discography has been reported in a high field system (Huang *et al*. 2002). In the study of Huang *et al*. it was concluded that MRI-discography could substitute conventional discography in selected indications. These indications would be allergy to ionated contrast or patients whose radiation exposure must be limited.

The contrast used in our study was gadolinium, which was diluted to saline in a ratio of 1 to 8. Gadolininum contrast is considered very safe and has long been used in intravascular applications with a low complication rate. There are no reports of toxic properties of gadolinium contrast towards any human tissue. Gadolinium contrast has not yet been approved for intrathecal use. In discography procedure there is a potential threat of intrathecal leagage of gadolinium. Gadolinium has been reported to have been used in animals and humans intrathecally without complications (Jinkins *et al*. 1999, Zeng *et al*. 1999). Having this information we proceeded with our study plan.

We had one complication reported in our study. The patient experienced continuous pain in the lumbar area after discography. The complication resulted in collapse of the disc space. Infectious agents were not found in laboratory cultivation and the exact etiology of disc collapse remained unknown. Discitis and disc collapse are well-known complications of discography procedure (Guyer *et al*. 1997, Junila *et al*. 1997) and in this respect, although unfortunate, it is concluded that the one complication does not challenge the feasibility of MR-guidance in performing discography. In this respect the role of prophylactic antibiotics in performing percutaneous discography cannot be underestimated (Osti *et al*. 1990).

Diagnostic MRI has surpassed conventional x-ray fluoroscopy and CT- discography as an imaging tool to assess disk morphology. MRI is efficient in pinpointing the pain sources of degenerative spine (Weishaupt *et al*. 2001). However, MRI also detects pathology in patients without symptoms. It is recognized that discography remains a good tool in providing the surgeon with information of the pain source by pointing out the disc level to be stabilized.

In our study we had a high procedural success rate showing MR-guidance to be feasible in discography. We had one procedural puncture failure and this puncture was targeted to collapsed intervertebral disk space at L5-to-S1 level. Our results show that pain response was adequately assessed in MR-guided puncture and injection, similarly to the principles in conventional discography. Pain provocation from the contrast injection could be graded as concordant or non-concordant. We did not grade pain intensity. The evaluation of concordant and non-concordant pain as well as pain intensity evaluation in discography is highly debated (Carragee 2000). However, there are also reports in favor of it (Walsh *et al*. 1990). It is felt that assessment of pain concordance is a key procedural element of discography and there is no replacement for it in evaluating discogenic pain. It must be noted that patients' emotional and chronic pain behavior has a strong affect on pain response in discography and such history in discography subject should be observed.

In our study the obtained MRI resolution of the injected contrast media appearing as an MRI discogram in intervertebral disc was less than that in conventional fluoroscopy. This could be due to diluted contrast and technical image formation factors in low field MRI or to the inherent physiological behavior of gadolininum contrast in vertebral disk where metabolism is distributed trough diffusion (Kerttula *et al*. 2000, Kurunlahti *et al*. 2001). Further evaluation of these factors was however out of scope of this study.

In this study the technique of MR-guided discography in low field scanner was presented and its feasibility discussed in interventional MRI and low field imaging surroundings. It is concluded that although the study has its restrictions in the form of a small amount of patients included in the study, it is shown that MR-guided discography is feasible and comparable to conventional discography. The use of MRI as a guidance method for discography also enables simultaneous conventional MRI data acquisition, thus broadening the possible diagnostic spectrum of the procedure.

It is apparent that further research with larger patient groups is warranted to determine the role of MR-guidance in discography.

6.6 MR-guided laser thermotherapy of osteiod osteoma

Osteioid osteoma is a benign lesion, that causes remarkably difficult symptoms and affects mainly young individuals at the peak of their physical activity. This sum-up leads to decreased level of physical activity, which can be very difficult both emotionally and physically for these patients and their families. Effective treatment of this benign lesion is challenging, not only because of the reasons mentioned above, but due to the fact that osteiod ostema frequently affects proximal or distal ends of long bones situating itself in the vicinity of chondral structures (Greenspan 1993). These lesions put great demands on operative surgery, which is the treatment of choice today in osteoid osteoma. Without image guidance the surgeon has to rely upon large amounts of regional bone tissue to be removed to be sure of complete removal of the nidus. If the nidus is located in the vicinity of joint structures this leads to long lasting (3 to 4 weeks) post-operative restrictions of stress and motor activity of the affected extremity, even if bone patch is used, placing further demands on the patient's endurance (Campanacci *et al*. 1999). The use of open surgical approach may also increase the risk of infectious operational complication.

Although percutaneous laser thermotherapy is considered a mini-invasive procedure, prophylactic antibiotics were used in our study. This was done with knowledge of the advantages of antibiotic prophylaxis in open orthopedic surgery (Norden 1991, Oishi *et al*. 1993, Mazza 2000). Infection complication associated with the percutaneous removal of osteoid osteoma has also been reported (Sans *et al*. 1999). The risk of an infection associated with the procedure was to be minimized.

Percutaneous interstitial laser treatment has been reported as an effective treatment for osteiod osteomas (Gangi *et al*. 1997a). With laser treatment tumor nidus is destroyed through heating. A defined volume of predictable size and shape can be obtained (Gangi *et al*. 1997c). This leaves the affected bone tissue volume significantly smaller than in surgical treatment without compromising the treatment effect. The smaller destruction area leads to little or no restrictions in extremity stress (max. one week) and thus shortens overall recovery time. Percutaneous approach is minimally invasive, and also diminishing damage to the skin and subcutaneous tissue, further favoring rapid recovery. With thermal destruction there is no need to support the destructed area since the damage to the cortical structures is usually minimal and even if coagulated, the destructed bone tissue has a filling effect on the area treated. This means that the diminishing effect of the treatment to the structural support delivered by the treated bone tissue is almost insignificant. Our results are in conclusion with earlier reports on interstitial laser treatment efficiency in treating osteid osteomas thus supporting the advantages of the percutaneous treatment approach over the surgical one.

Different therapeutic methods of osteoid osteoma and their results are demonstrated in Table 9.

Table 9. Different therapeutic methods of osteoid osteoma and their results.

Method	Success rate%	n	Author
RF	76	97	(Vanderschueren *et al.* 2002)
Operation	86.7	105	(Yildiz *et al.* 2001)
RF	94	47	(Woertler *et al.* 2001)
RF	95	58	(Lindner *et al.* 2001)
Laser	95	23	(Witt *et al.* 2000)
Percutaneous resection	84	38	(Sans *et al.* 1999)
RF	88	3	(Rosenthal *et al.* 1998)
Laser	93	15	(Gangi *et al.* 1997a)
Laser	95	22	(Gangi *et al.* 1997b)
Percutaneous excision	87.5	16	(Roger *et al.* 1996)
Laser	94	18	(de Berg *et al.* 1995)

In our study we used MRI for lesion localization, instrument guidance and treatment monitoring.

The spatial resolution of MRI in bone is good, the nidus of osteiod osteoma can be reliably recognized (Spouge & Thain 2000) and thus targeted in MRI. This was also shown in our study, where all the lesions were detected in the low-field scanner used. The unique ability of MRI is its capability to monitor thermal changes in tissue. This is not possible to the same extent with CT or ultrasound, only MRI can provide quantitative information about thermal changes in tissue (Vogl *et al.* 1997, Eyrich *et al.* 2000, Germain *et al.* 2001a, Germain *et al.* 2001b, Wohlgemuth *et al.* 2001). In our study we used modified CBASS sequence to image treated area during laser ablation. The CBASS sequence used was constructed to facilitate the detection of possible change in T1 relaxation time and related signal void caused by increasing temperature in tissue as reported earlier (Germain *et al.* 2002). Although all the lesions were reliably identified for puncture, reliable signal change correlating to the temperature change during treatment was not detected with the thermal sequence used. This could be due to an already weak signal from cortical bone, which the majority of the osteoid consists of. Another reason for low signal change may be the failure to optimize sequence properties for bone tissue. The use of thinner slices for imaging may be the key to overcome this problem. Although the inability to detect signal change can be considered failure, one can be optimistic that further optimization of sequence protocols will yield better results in thermal monitoring in low field surroundings in future. As a backup we calculated the maximum energy deliverable to the lesion area using a formula calculated from the experimental study results conducted in pigs (Gangi *et al.* 1997c). From the results of that study a linear model of delivered energy amounts in relation to the size of tissue necrosis could be acquired. By applying the nidus size of osteoma to this model a maximal energy amount deliverable could be determined. We had one recurrent osteid osteoma in our study during the 6-month follow-up. The patient had an untypical large osteiod osteoma nidus (2 cm) and this may be the key to the failure, even though two laser fibers were used to achieve destruction of the nidus. The patient was retreated with laser ablation and was again symptom and complication free 3 weeks after the repeated procedure.

Although there was a recurrent osteoid osteoma in our patient data, this study demonstrates the preliminary feasibility of MRI in guiding percutaneous interstitial laser ablation treatment of osteoid osteomas. MRI can be used as a solo guidance modality for this procedure and is in this respect comparable to CT.

7 Conclusions

1. The optical guidance method in conjunction with MR-guidance in bone biopsies provides precise and safe instrument control during MR-guided procedure at 0.23 T.
2. MR-guidance in performing bone biopsies is clinically viable in various anatomical areas at 0.23 T.
3. MR-guided nerve root therapies are safe and the same therapeutic effect as with conventional guidance methods can be achieved under MR- guidance at 0.23T.
4. MR-guided discography can be adequately performed at 0.23T.
5. Thermal laser therapy in treating osteoid osteoma is feasible under MR-guidance at 0.23 T.

8 References

Adam G, Bucker A, Nolte-Ernsting C, Tacke J & Gunther RW (1999) Interventional MR imaging: percutaneous abdominal and skeletal biopsies and drainages of the abdomen. Eur Radiol 9(8): 1471-8.

Anderson SR & Flanagan B (2000) Discography. Curr Rev Pain 4(5): 345-52.

Arthur WR, Dhawan J, Norell MS, Hunter AJ & Clark AL (2002) Does cardiologist- or radiographer-operated fluoroscopy and image acquisition influence optimization of patient radiation exposure during routine coronary angiography? Br J Radiol 75(897): 748-53.

Assoun J, Richardi G, Railhac JJ, Baunin C, Fajadet P, Giron J, Maquin P, Haddad J & Bonnevialle P (1994) Osteoid osteoma: MR imaging versus CT. Radiology 191(1): 217-23.

Bakker CJ, Hoogeveen RM, Weber J, van Vaals JJ, Viergever MA & Mali WP (1996) Visualization of dedicated catheters using fast scanning techniques with potential for MR-guided vascular interventions. Magn Reson Med 36(6): 816-20.

Barei DP, Moreau G, Scarborough MT & Neel MD (2000) Percutaneous radiofrequency ablation of osteoid osteoma. Clin Orthop(373): 115-24.

Barnett GH, Kormos DW, Steiner CP & Weisenberger J (1993) Use of a frameless, armless stereotactic wand for brain tumor localization with two-dimensional and three-dimensional neuroimaging. Neurosurgery 33(4): 674-8.

Boden SD, Davis DO, Dina TS, Patronas NJ & Wiesel SW (1990) Abnormal magnetic-resonance scans of the lumbar spine in asymptomatic subjects. A prospective investigation. J Bone Joint Surg Am 72(3): 403-8.

Buecker A, Adam G, Neuerburg JM, Glowinski A, van Vaals JJ & Guenther RW (1998) MR-guided biopsy using a T2-weighted single-shot zoom imaging sequence (Local Look technique). J Magn Reson Imaging 8(4): 955-9.

Buecker A, Neuerburg JM, Adam GB, Nolte-Ernsting CC, Hunter DW, Glowinski A, van Vaals JJ & Guenther RW (2001) MR-guided percutaneous drainage of abdominal fluid collections in combination with X-ray fluoroscopy: initial clinical experience. Eur Radiol 11(4): 670-4.

Busch M, Bornstedt A, Wendt M, Duerk JL, Lewin JS & Gronemeyer D (1998) Fast "real time" imaging with different k-space update strategies for interventional procedures. J Magn Reson Imaging 8(4): 944-54.

Butts K, Pauly JM, Daniel BL, Kee S & Norbash AM (1999) Management of biopsy needle artifacts: techniques for RF-refocused MRI. J Magn Reson Imaging 9(4): 586-95.

Campanacci M, Ruggieri P, Gasbarrini A, Ferraro A & Campanacci L (1999) Osteoid osteoma. Direct visual identification and intralesional excision of the nidus with minimal removal of bone. J Bone Joint Surg Br 81(5): 814-20.

Carragee EJ (2000) Is lumbar discography a determinate of discogenic low back pain: provocative discography reconsidered. Curr Rev Pain 4(4): 301-8.

Caversaccio M, Bachler R, Ladrach K, Schroth G, Nolte LP & Hausler R (1999) The "Bernese" frameless optical computer aided surgery system. Comput Aided Surg 4(6): 328-34.

Cerase A & Priolo F (1998) Skeletal benign bone-forming lesions. Eur J Radiol 27(Suppl 1): S91-7.

Cline HE, Schenck JF, Hynynen K, Watkins RD, Souza SP & Jolesz FA (1992) MR-guided focused ultrasound surgery. J Comput Assist Tomogr 16(6): 956-65.

Cove JA, Taminiau AH, Obermann WR & Vanderschueren GM (2000) Osteoid osteoma of the spine treated with percutaneous computed tomography-guided thermocoagulation. Spine 25(10): 1283-6.

de Berg JC, Pattynama PM, Obermann WR, Bode PJ, Vielvoye GJ & Taminiau AH (1995) Percutaneous computed-tomography-guided thermocoagulation for osteoid osteomas. Lancet 346(8971): 350-1.

de Jode MG, Vale JA & Gedroyc WM (1999) MR-guided laser thermoablation of inoperable renal tumors in an open-configuration interventional MR scanner: preliminary clinical experience in three cases. J Magn Reson Imaging 10(4): 545-9.

Derby R, Howard MW, Grant JM, Lettice JJ, Van Peteghem PK & Ryan DP (1999) The ability of pressure-controlled discography to predict surgical and nonsurgical outcomes. Spine 24(4): 364-71; discussion 371-2.

Derby R, Kine G, Saal JA, Reynolds J, Goldthwaite N, White AH, Hsu K & Zucherman J (1992) Response to steroid and duration of radicular pain as predictors of surgical outcome. Spine 17(6 Suppl): S176-83.

Dick EA, Taylor-Robinson SD, Thomas HC & Gedroyc WM (2002) Ablative therapy for liver tumours. Gut 50(5): 733-9.

Dotter CT & Judkins MP (1964) Transluminar treatment of arteriosclerotic obstuctions: descriptions of a new technique and a preliminary report of its application. Circulation 30: 654-77.

Duckwiler G, Lufkin RB & Hanafee WN (1989) MR-directed needle biopsies. Radiol Clin North Am 27(2): 255-63.

Duerk JL, Lewin JS, Wendt M & Petersilge C (1998) Remember true FISP? A high SNR, near 1-second imaging method for T2-like contrast in interventional MRI at .2 T. J Magn Reson Imaging 8(1): 203-8.

Duerk JL, Lewin JS & Wu DH (1996) Application of keyhole imaging to interventional MRI: a simulation study to predict sequence requirements. J Magn Reson Imaging 6(6): 918-24.

Ehnholm GJ, Vahala ET, Kinnunen J, Nieminen JE, Standertskjold-Nordenstam C & Uusitalo MA (1999) Electron spin resonance (ESR) probe for interventional MRI instrument localization. J Magn Reson Imaging 10(2): 216-9.

Eyrich GK, Bruder E, Hilfiker P, Dubno B, Quick HH, Patak MA, Gratz KW & Sailer HF (2000) Temperature mapping of magnetic resonance-guided laser interstitial thermal therapy (LITT) in lymphangiomas of the head and neck. Lasers Surg Med 26(5): 467-76.

Fiedler VU, Schwarzmaier HJ, Eickmeyer F, Muller FP, Schoepp C & Verreet PR (2001) Laser-induced interstitial thermotherapy of liver metastases in an interventional 0.5 Tesla MRI system: technique and first clinical experiences. J Magn Reson Imaging 13(5): 729-37.

Fraser-Hill MA, Renfrew DL & Hilsenrath PE (1992) Percutaneous needle biopsy of musculoskeletal lesions. 2. Cost-effectiveness. AJR Am J Roentgenol 158(4): 813-8.

Frymoyer JW & Cats-Baril WL (1991) An overview of the incidences and costs of low back pain. Orthop Clin North Am 22(2): 263-71.

Gangi A, Dietemann JL, Gasser B, Mortazavi R, Brunner P, Mourou MY, Dosch JC, Durckel J, Marescaux J & Roy C (1997a) Interstitial laser photocoagulation of osteoid osteomas with use of CT guidance. Radiology 203(3): 843-8.

Gangi A, Dietemann JL, Gasser B, Mortazavi R, Dosch JC, Dupuis M, Durckel J & Roy C (1997b) Percutaneous Laser Photocoagulation of Osteoid Osteomas. Semin Musculoskelet Radiol 1(2): 273-280.

Gangi A, Gasser B, De Unamuno S, Fogarrassy E, Fuchs C, Siffert P, Dietemann JL & Roy C (1997c) New Trends in Interstitial Laser Photocoagulation of Bones. Semin Musculoskelet Radiol 1(2): 331-338.

Geirnaerdt MJ, Bloem JL, van der Woude HJ, Taminiau AH, Nooy MA & Hogendoorn PC (1998) Chondroblastic osteosarcoma: characterisation by gadolinium-enhanced MR imaging correlated with histopathology. Skeletal Radiol 27(3): 145-53.

Genant JW, Vandevenne JE, Bergman AG, Beaulieu CF, Kee ST, Norbash AM & Lang P (2002) Interventional musculoskeletal procedures performed by using MR imaging guidance with a vertically open MR unit: assessment of techniques and applicability. Radiology 223(1): 127-36.

Germain D, Chevallier P, Laurent A & Saint-Jalmes H (2001a) MR monitoring of tumour thermal therapy. Magma 13(1): 47-59.

Germain D, Chevallier P, Laurent A, Savart M, Wassef M & Saint-Jalmes H (2001b) MR monitoring of laser-induced lesions of the liver in vivo in a low-field open magnet: temperature mapping and lesion size prediction. J Magn Reson Imaging 13(1): 42-9.

Germain D, Vahala E, Ehnholm GJ, Vaara T, Ylihautala M, Savart M, Laurent A, Tanttu J & Saint-Jalmes H (2002) MR temperature measurement in liver tissue at 0.23 T with a steady-state free precession sequence. Magn Reson Med 47(5): 940-7.

Glowinski A, Kursch J, Adam G, Bucker A, Noll TG & Gunther RW (1998) Device visualization for interventional MRI using local magnetic fields: basic theory and its application to catheter visualization. IEEE Trans Med Imaging 17(5): 786-93.

Greenspan A (1993) Benign bone-forming lesions: osteoma, osteoid osteoma, and osteoblastoma. Clinical, imaging, pathologic, and differential considerations. Skeletal Radiol 22(7): 485-500.

Gronemeyer DH, Schirp S & Gevargez A (2002) Image-guided radiofrequency ablation of spinal tumors: preliminary experience with an expandable array electrode. Cancer J 8(1): 33-9.

Gronemeyer DH, Seibel RM & Kaufman L (1991) Low-field design eases MRI-guided biopsies. Diagn Imaging (San Franc) 13(3): 139-43.

Gronvall J, Gronvall S & Hegedus V (1977) Ultrasound-guided drainage of fluid-containing masses using angiographic catheterization techniques. AJR Am J Roentgenol 129(6): 997-1002.

Guyer RD, Ohnmeiss DD, Mason SL & Shelokov AP (1997) Complications of cervical discography: findings in a large series. J Spinal Disord 10(2): 95-101.

Haschek E & Lindenthal O (1896) A contribution to the practical use of the photography according to Röntgen. In: Stanley Baum, editor, Abrams' Angiography. Boston: Little, Brown and Company; 1997, p 3.

Heid O, Deimling M & Huk WJ (1995) Ultra-rapid gradient echo imaging. Magn Reson Med 33(1): 143-9.

Heywang-Kobrunner SH, Heinig A, Schaumloffel U, Viehweg P, Buchmann J, Lampe D & Spielmann R (1999) MR-guided percutaneous excisional and incisional biopsy of breast lesions. Eur Radiol 9(8): 1656-65.

Hinks RS, Bronskill MJ, Kucharczyk W, Bernstein M, Collick BD & Henkelman RM (1998) MR systems for image-guided therapy. J Magn Reson Imaging 8(1): 19-25.

Hoane BR, Shields AF, Porter BA & Shulman HM (1991) Detection of lymphomatous bone marrow involvement with magnetic resonance imaging. Blood 78(3): 728-38.

Holm HH, Kristensen JK, Rasmussen SN, Northeved A & Barlebo H (1972) Ultrasound as a guide in percutaneous puncture technique. Ultrasonics 10(2): 83-6.

Huang TS, Zucherman JF, Hsu KY, Shapiro M, Lentz D & Gartland J (2002) Gadopentetate dimeglumine as an intradiscal contrast agent. Spine 27(8): 839-43.

Huppert PE, Trubenbach J, Schick F, Pereira P, Konig C & Claussen CD (2000) [MRI-guided percutaneous radiofrequency ablation of hepatic neoplasms--first technical and clinical experiences]. Rofo Fortschr Geb Rontgenstr Neuen Bildgeb Verfahr 172(8): 692-700.

Hynynen K, Pomeroy O, Smith DN, Huber PE, McDannold NJ, Kettenbach J, Baum J, Singer S & Jolesz FA (2001) MR imaging-guided focused ultrasound surgery of fibroadenomas in the breast: a feasibility study. Radiology 219(1): 176-85.

Jacob AL, Messmer P, Kaim A, Suhm N, Regazzoni P & Baumann B (2000) A whole-body registration-free navigation system for image-guided surgery and interventional radiology. Invest Radiol 35(5): 279-88.

Jager L & Reiser M (2001) CT and MR imaging of the normal and pathologic conditions of the facial nerve. Eur J Radiol 40(2): 133-46.

Jelinek JS, Kransdorf MJ, Gray R, Aboulafia AJ & Malawer MM (1996) Percutaneous transpedicular biopsy of vertebral body lesions. Spine 21(17): 2035-40.

Jenkins LT, Millikan KW, Bines SD, Staren ED & Doolas A (1997) Hepatic resection for metastatic colorectal cancer. Am Surg 63(7): 605-10.

Jensen MC, Brant-Zawadzki MN, Obuchowski N, Modic MT, Malkasian D & Ross JS (1994) Magnetic resonance imaging of the lumbar spine in people without back pain. N Engl J Med 331(2): 69-73.

Jinkins JR, Williams RF & Xiong L (1999) Evaluation of gadopentetate dimeglumine magnetic resonance cisternography in an animal model: preliminary report. Invest Radiol 34(2): 156-9.

Joensuu RP, Sepponen RE, Lamminen AE & Standertskjold-Nordenstam CG (2000) A shielded Overhauser marker for MR tracking of interventional devices. Magn Reson Med 43(1): 139-45.

Jolesz FA (1998) Interventional and intraoperative MRI: a general overview of the field. J Magn Reson Imaging 8(1): 3-7.

Jolesz FA & Blumenfeld SM (1994) Interventional use of magnetic resonance imaging. Magn Reson Q 10(2): 85-96.

Jolesz FA, Hynynen K, Pomeroy O, Smith DN, Huber PE, McDannold NJ, Kettenbach J, Baum J & Singer S (2002) Magnetic resonance image-guided focused ultrasound surgery

MR imaging-guided focused ultrasound surgery of fibroadenomas in the breast: a feasibility study. Cancer J 8(Suppl 1): S100-12.

Junila J, Niinimaki T & Tervonen O (1997) Epidural abscess after lumbar discography. A case report. Spine 22(18): 2191-3.

Jyrkinen L, Ojala R, Haataja L, Blanco Sequeiros R, Klemola R, Silven O & Tervonen O (2000) Managing the Complexity of the User Interface of a MRI Guided Surgery System. In: Proceedings of the 6th ERCIM Workshop "user interfaces for All", Florence: 213-9.

Kaplan GR, Saifuddin A, Pringle JA, Noordeen MH & Mehta MH (1998) Langerhans' cell histiocytosis of the spine: use of MRI in guiding biopsy. Skeletal Radiol 27(12): 673-6.

Karppinen J, Malmivaara A, Kurunlahti M, Kyllonen E, Pienimaki T, Nieminen P, Ohinmaa A, Tervonen O & Vanharanta H (2001) Periradicular infiltration for sciatica: a randomized controlled trial. Spine 26(9): 1059-67.

Kerttula LI, Jauhiainen JP, Tervonen O, Suramo IJ, Koivula A & Oikarinen JT (2000) Apparent diffusion coefficient in thoracolumbar intervertebral discs of healthy young volunteers. J Magn Reson Imaging 12(2): 255-60.

Kettenbach J, Kacher DF, Koskinen SK, Silverman SG, Nabavi A, Gering D, Tempany CM, Schwartz RB, Kikinis R, Black PM & Jolesz FA (2000) Interventional and intraoperative magnetic resonance imaging. Annu Rev Biomed Eng 2: 661-90.

Koenig CW, Duda SH, Truebenbach J, Schott UG, Maurer F, Claussen CD & Pereira PL (2001) MR-guided biopsy of musculoskeletal lesions in a low-field system. J Magn Reson Imaging 13(5): 761-8.

Konings MK, Bartels LW, van Swol CF & Bakker CJ (2001) Development of an MR-safe tracking catheter with a laser-driven tip coil. J Magn Reson Imaging 13(1): 131-5.

Kransdorf MJ, Stull MA, Gilkey FW & Moser RP, Jr. (1991) Osteoid osteoma. Radiographics 11(4): 671-96.

Krempen JF, Smith BS & DeFreest LJ (1975) Selective nerve root infiltration for the evaluation of sciatica. Orthop Clin North Am 6(1): 311-5.

Kurunlahti M, Kerttula L, Jauhiainen J, Karppinen J & Tervonen O (2001) Correlation of diffusion in lumbar intervertebral disks with occlusion of lumbar arteries: a study in adult volunteers. Radiology 221(3): 779-86.

Ladd ME, Zimmermann GG, Quick HH, Debatin JF, Boesiger P, von Schulthess GK & McKinnon GC (1998) Active MR visualization of a vascular guidewire in vivo. J Magn Reson Imaging 8(1): 220-5.

Laufer U, Kirchner J, Kickuth R, Adams S, Jendreck M & Liermann D (2001) A comparative study of CT fluoroscopy combined with fluoroscopy versus fluoroscopy alone for percutaneous transhepatic biliary drainage. Cardiovasc Intervent Radiol 24(4): 240-4.

Law P & Regan L (2000) Interstitial thermo-ablation under MRI guidance for the treatment of fibroids. Curr Opin Obstet Gynecol 12(4): 277-82.

Leffler SG & Chew FS (1999) CT-guided percutaneous biopsy of sclerotic bone lesions: diagnostic yield and accuracy. AJR Am J Roentgenol 172(5): 1389-92.

Lewin JS, Duerk JL, Jain VR, Petersilge CA, Chao CP & Haaga JR (1996) Needle localization in MR-guided biopsy and aspiration: effects of field strength, sequence design, and magnetic field orientation. AJR Am J Roentgenol 166(6): 1337-45.

Lewin JS, Petersilge CA, Hatem SF, Duerk JL, Lenz G, Clampitt ME, Williams ML, Kaczynski KR, Lanzieri CF, Wise AL & Haaga JR (1998) Interactive MR imaging-guided biopsy and aspiration with a modified clinical C-arm system. AJR Am J Roentgenol 170(6): 1593-601.

Lindner NJ, Ozaki T, Roedl R, Gosheger G, Winkelmann W & Wortler K (2001) Percutaneous radiofrequency ablation in osteoid osteoma. J Bone Joint Surg Br 83(3): 391-6.

Livraghi T (2001) Percutaneous ethanol injection in the treatment of hepatocellular carcinoma in cirrhosis. Hepatogastroenterology 48(37): 20-4.

Livraghi T, Goldberg SN, Lazzaroni S, Meloni F, Ierace T, Solbiati L & Gazelle GS (2000) Hepatocellular carcinoma: radio-frequency ablation of medium and large lesions. Radiology 214(3): 761-8.

Lufkin R, Teresi L, Chiu L & Hanafee W (1988) A technique for MR-guided needle placement. AJR Am J Roentgenol 151(1): 193-6.

Lufkin R, Teresi L & Hanafee W (1987) New needle for MR-guided aspiration cytology of the head and neck. AJR Am J Roentgenol 149(2): 380-2.

Lutz GE, Vad VB & Wisneski RJ (1998) Fluoroscopic transforaminal lumbar epidural steroids: an outcome study. Arch Phys Med Rehabil 79(11): 1362-6.

Mala T, Edwin B, Samset E, Gladhaug I, Hol PK, Fosse E, Mathisen O, Bergan A & Soreide O (2001) Magnetic-resonance-guided percutaneous cryoablation of hepatic tumours. Eur J Surg 167(8): 610-7.

Mankin HJ, Lange TA & Spanier SS (1982) The hazards of biopsy in patients with malignant primary bone and soft-tissue tumors. J Bone Joint Surg [Am] 64(8): 1121-7.

Martino CR, Haaga JR, Bryan PJ, LiPuma JP, El Yousef SJ & Alfidi RJ (1984) CT-guided liver biopsies: eight years' experience. Work in progress. Radiology 152(3): 755-7.

Matsumoto R, Selig AM, Colucci VM & Jolesz FA (1992) Interstitial Nd:YAG laser ablation in normal rabbit liver: trial to maximize the size of laser-induced lesions. Lasers Surg Med 12(6): 650-8.

Mazza A (2000) Ceftriaxone as short-term antibiotic prophylaxis in orthopedic surgery: a cost-benefit analysis involving 808 patients. J Chemother 12 Suppl 3: 29-33.

McParland BJ (1998) A study of patient radiation doses in interventional radiological procedures. Br J Radiol 71(842): 175-85.

Midorikawa T, Kumada K, Kikuchi H, Ishibashi K, Yagi H, Nagasaki H, Nemoto H, Saitoh M, Nakano H, Yamaguchi M, Koh Y, Sakai H, Yoshizawa Y, Sanada Y & Yoshiba M (2000) Microwave coagulation therapy for hepatocellular carcinoma. J Hepatobiliary Pancreat Surg 7(3): 252-9.

Mink JH, Deutsch AL, Goldstein TB, Bray R, Pashman R, Armstrong, II, Sinel M & Gart A (1998) Spinal imaging and intervention: 1998. Phys Med Rehabil Clin N Am 9(2): 343-80, viii.

Morvan D, Leroy-Willig A, Malgouyres A, Cuenod CA, Jehenson P & Syrota A (1993) Simultaneous temperature and regional blood volume measurements in human muscle using an MRI fast diffusion technique. Magn Reson Med 29(3): 371-7.

Mueller PR, Stark DD, Simeone JF, Saini S, Butch RJ, Edelman RR, Wittenberg J & Ferrucci JT, Jr. (1986) MR-guided aspiration biopsy: needle design and clinical trials. Radiology 161(3): 605-9.

Murphy WA & Totty WG (1986) Musculoskeletal magnetic resonance imaging. Magn Reson Annu: 1-35.

Narozny M, Zanetti M & Boos N (2001) Therapeutic efficacy of selective nerve root blocks in the treatment of lumbar radicular leg pain. Swiss Med Wkly 131(5-6): 75-80.

Neeleman N, Wobbes T, Jager GJ & Ruers TJ (2001) Cryosurgery as treatment modality for colorectal liver metastases. Hepatogastroenterology 48(38): 325-9.

Neuerburg J, Adam G, Bucker A, Zilkens KW, Schmitz-Rode T, Katterbach FJ, Klosterhalfen B, Rasmussen E, van Vaals JJ & Gunther RW (1998a) [A new MR-(and CT-) compatible bone biopsy system: first clinical results]. Rofo Fortschr Geb Rontgenstr Neuen Bildgeb Verfahr 169(5): 515-20.

Neuerburg JM, Adam G, Buecker A, Zilkens KW, Schmitz-Rode T, Hunter D, van Vaals JJ & Guenther RW (1998b) MRI-guided biopsy of bone in a hybrid system. J Magn Reson Imaging 8(1): 85-90.

Ng CS, Salisbury JR, Darby AJ & Gishen P (1998) Radiologically guided bone biopsy: results of 502 biopsies. Cardiovasc Intervent Radiol 21(2): 122-8.

Norden CW (1991) Antibiotic prophylaxis in orthopedic surgery. Rev Infect Dis 13 Suppl 10: S842-6.

Oishi CS, Carrion WV & Hoaglund FT (1993) Use of parenteral prophylactic antibiotics in clean orthopaedic surgery. A review of the literature. Clin Orthop(296): 249-55.

Ojala R, Klemola R, Karppinen J, Sequeiros RB & Tervonen O (2001) Sacro-iliac joint arthrography in low back pain: feasibility of MRI guidance. Eur J Radiol 40(3): 236-9.

Ojala R, Vahala E, Karppinen J, Klemola R, Blanco-Sequeiros R, Vaara T & Tervonen O (2000) Nerve root infiltration of the first sacral root with MRI guidance. J Magn Reson Imaging 12(4): 556-61.

Osti OL, Fraser RD & Vernon-Roberts B (1990) Discitis after discography. The role of prophylactic antibiotics. J Bone Joint Surg Br 72(2): 271-4.

Parkkola RK, Mattila KT, Heikkila JT, Ekfors TO, Kallajoki MA, Komu ME, Vaara TJ & Aro HT (2001) Dynamic contrast-enhanced MR imaging and MR-guided bone biopsy on a 0.23 T open imager. Skeletal Radiol 30(11): 620-4.

Paulson EK, Sheafor DH, Enterline DS, McAdams HP & Yoshizumi TT (2001) CT fluoroscopy--guided interventional procedures: techniques and radiation dose to radiologists. Radiology 220(1): 161-7.

Pedersen EM, Stenbog EV, Frund T, Houlind K, Kromann O, Sorensen KE, Emmertsen K & Hjortdal VE (2002) Flow during exercise in the total cavopulmonary connection measured by magnetic resonance velocity mapping. Heart 87(6): 554-8.

Perlet C, Schneider P, Amaya B, Grosse A, Sittek H, Reiser MF & Heywang-Kobrunner SH (2002) MR-Guided vacuum biopsy of 206 contrast-enhancing breast lesions. Rofo Fortschr Geb Rontgenstr Neuen Bildgeb Verfahr 174(1): 88-95.

Pfirrmann CW, Oberholzer PA, Zanetti M, Boos N, Trudell DJ, Resnick D & Hodler J (2001) Selective nerve root blocks for the treatment of sciatica: evaluation of injection site and effectiveness--a study with patients and cadavers. Radiology 221(3): 704-11.

Popowski Y, Hiltbrand E, Joliat D & Rouzaud M (2000) Open magnetic resonance imaging using titanium-zirconium needles: improved accuracy for interstitial brachytherapy implants? Int J Radiat Oncol Biol Phys 47(3): 759-65.

Quesson B, de Zwart JA & Moonen CT (2000) Magnetic resonance temperature imaging for guidance of thermotherapy. J Magn Reson Imaging 12(4): 525-33.

Quesson B, Vimeux F, Salomir R, De Zwart JA & Moonen CT (2002) Automatic control of hyperthermic therapy based on real-time Fourier analysis of MR temperature maps. Magn Reson Med 47(6): 1065-72.

Radcliffe SN, Walsh HJ & Carty H (1998) Osteoid osteoma: the difficult diagnosis. Eur J Radiol 28(1): 67-79.

Roger B, Bellin MF, Wioland M & Grenier P (1996) Osteoid osteoma: CT-guided percutaneous excision confirmed with immediate follow-up scintigraphy in 16 outpatients. Radiology 201(1): 239-42.

Rohling R, Munger P, Hollerbach JM & Peter T (1995) Comparison of relative accuracy between a mechanical and an optical position tracker for image-guided neurosurgery. J Image Guid Surg 1(1): 30-4.

Rordorf G, Koroshetz WJ, Copen WA, Cramer SC, Schaefer PW, Budzik RF, Jr., Schwamm LH, Buonanno F, Sorensen AG & Gonzalez G (1998) Regional ischemia and ischemic injury in patients with acute middle cerebral artery stroke as defined by early diffusion-weighted and perfusion-weighted MRI. Stroke 29(5): 939-43.

Rosenthal DI, Hornicek FJ, Wolfe MW, Jennings LC, Gebhardt MC & Mankin HJ (1998) Percutaneous radiofrequency coagulation of osteoid osteoma compared with operative treatment. J Bone Joint Surg Am 80(6): 815-21.

Sachs BL, Vanharanta H, Spivey MA, Guyer RD, Videman T, Rashbaum RF, Johnson RG, Hochschuler SH & Mooney V (1987) Dallas discogram description. A new classification of CT/discography in low-back disorders. Spine 12(3): 287-94.

Saifuddin A, Mitchell R, Burnett SJ, Sandison A & Pringle JA (2000) Ultrasound-guided needle biopsy of primary bone tumours. J Bone Joint Surg Br 82(1): 50-4.

Salomonowitz E (2001) MR imaging-guided biopsy and therapeutic intervention in a closed-configuration magnet: single-center series of 361 punctures. AJR Am J Roentgenol 177(1): 159-63.

Salomonowitz EK, Cejna M & Dewey C (2000) Simple and effective technique of guided biopsy in a closed MRI system. Abdom Imaging 25(6): 638-42.

Sans N, Galy-Fourcade D, Assoun J, Jarlaud T, Chiavassa H, Bonnevialle P, Railhac N, Giron J, Morera-Maupome H & Railhac JJ (1999) Osteoid osteoma: CT-guided percutaneous resection and follow-up in 38 patients. Radiology 212(3): 687-92.

Schafroth E, Saltzman J & Probst P (1987) [Real-time sonography of cholangiolithiasis. Dependence of the diagnostic accuracy on the competence of the operator]. ROFO Fortschr Geb Rontgenstr Nuklearmed 147(3): 307-9.

Schenck JF, Jolesz FA, Roemer PB, Cline HE, Lorensen WE, Kikinis R, Silverman SG, Hardy CJ, Barber WD, Laskaris ET & et al. (1995) Superconducting open-configuration MR imaging system for image-guided therapy. Radiology 195(3): 805-14.

Seibel RM, Melzer A, Schmidt A & Plabetamann J (1997) Computed Tomography- and Magnetic Resonance Imaging: Guided Microtherapy. Semin Laparosc Surg 4(2): 61-73.

Seifert JK, Bottger TC, Weigel TF, Gonner U & Junginger T (2000) Prognostic factors following liver resection for hepatic metastases from colorectal cancer. Hepatogastroenterology 47(31): 239-46.

Settle WJ, Ebraheim NA, Coombs R, Saunders RC & Jackson WT (1990) CT-guided biopsy of metastatic sacral tumors. Orthopedics 13(7): 753-8.

Shankman S, Desai P & Beltran J (1997) Subperiosteal osteoid osteoma: radiographic and pathologic manifestations. Skeletal Radiol 26(8): 457-62.

Silverman SG, Collick BD, Figueira MR, Khorasani R, Adams DF, Newman RW, Topulos GP & Jolesz FA (1995) Interactive MR-guided biopsy in an open-configuration MR imaging system. Radiology 197(1): 175-81.

Silverman SG, Tuncali K, Adams DF, Nawfel RD, Zou KH & Judy PF (1999) CT fluoroscopy-guided abdominal interventions: techniques, results, and radiation exposure. Radiology 212(3): 673-81.

Smits HF, Bos C, van der Weide R & Bakker CJ (1999) Interventional MR: vascular applications. Eur Radiol 9(8): 1488-95.

Smyczek-Gargya B, Krainick U, Muller-Schimpfle M, Mielke G, Mayer R, Siegmann K, Mehnert F, Vogel U, Ruck P, Wallwiener D & Fersis N (2002) Large-core needle biopsy for diagnosis and treatment of breast lesions. Arch Gynecol Obstet 266(4): 198-200.

Sodickson DK, Griswold MA & Jakob PM (1999) SMASH imaging. Magn Reson Imaging Clin N Am 7(2): 237-54, vii-viii.

Solbiati L, Livraghi T, Goldberg SN, Ierace T, Meloni F, Dellanoce M, Cova L, Halpern EF & Gazelle GS (2001) Percutaneous radio-frequency ablation of hepatic metastases from colorectal cancer: long-term results in 117 patients. Radiology 221(1): 159-66.

Sones PJ (1984) Percutaneous drainage of abdominal abscesses. AJR Am J Roentgenol 142(1): 35-9.

Spouge AR & Thain LM (2000) Osteoid osteoma: MR imaging revisited. Clin Imaging 24(1): 19-27.

Tanaka T, Inaba Y, Arai Y, Matsueda K, Aramaki T & Dendo S (2002) Mediastinal abscess successfully treated by percutaneous drainage using a unified CT and fluoroscopy system. Br J Radiol 75(893): 470-3.

Tang S, Li JH, Lui SL, Chan TM, Cheng IK & Lai KN (2002) Free-hand, ultrasound-guided percutaneous renal biopsy: experience from a single operator. Eur J Radiol 41(1): 65-9.

Teeuwisse WM, Geleijns J, Broerse JJ, Obermann WR & van Persijn van Meerten EL (2001) Patient and staff dose during CT guided biopsy, drainage and coagulation. Br J Radiol 74(884): 720-6.

Tehranzadeh J (1998) Discography 2000. Radiol Clin North Am 36(3): 463-95.

Tikkakoski T, Lahde S, Puranen J & Apaja-Sarkkinen M (1992) Combined CT-guided biopsy and cytology in diagnosis of bony lesions. Acta Radiol 33(3): 225-9.

Tung GA & Davis LM (1993) The role of magnetic resonance imaging in the evaluation of the soft tissue mass. Crit Rev Diagn Imaging 34(5): 239-308.

Uhlenbrock D & Arlinghaus J (1997) [Results of CT-guided periradicular pain therapy]. Rofo Fortschr Geb Rontgenstr Neuen Bildgeb Verfahr 166(6): 528-34.

Vahala E, Ylihautala M, Tuominen J, Schiffbauer H, Katisko J, Yrjana S, Vaara T, Ehnholm G & Koivukangas J (2001) Registration in interventional procedures with optical navigator. J Magn Reson Imaging 13(1): 93-8.

Vamvanij V, Fredrickson BE, Thorpe JM, Stadnick ME & Yuan HA (1998) Surgical treatment of internal disc disruption: an outcome study of four fusion techniques. J Spinal Disord 11(5): 375-82.

Vanderschueren GM, Taminiau AH, Obermann WR & Bloem JL (2002) Osteoid osteoma: clinical results with thermocoagulation. Radiology 224(1): 82-6.

vanSonnenberg E, Hajek P, Gylys-Morin V, Varney RA, Baker L, Casola G, Christensen R & Mattrey RF (1988) A wire-sheath system for MR-guided biopsy and drainage: laboratory studies and experience in 10 patients. AJR Am J Roentgenol 151(4): 815-7.

Vehmas T (1997) Radiation exposure during standard and complex interventional procedures. Br J Radiol 70: 296-8.

Viton JM, Peretti-Viton P, Rubino T, Delarque A & Salamon N (1998) Short-term assessment of periradicular corticosteroid injections in lumbar radiculopathy associated with disc pathology. Neuroradiology 40(1): 59-62.

Vogl TJ, Mack MG, Muller PK, Straub R, Engelmann K & Eichler K (1999a) Interventional MR: interstitial therapy. Eur Radiol 9(8): 1479-87.

Vogl TJ, Mack MG, Roggan A, Straub R, Eichler KC, Muller PK, Knappe V & Felix R (1998) Internally cooled power laser for MR-guided interstitial laser-induced thermotherapy of liver lesions: initial clinical results. Radiology 209(2): 381-5.

Vogl TJ, Mack MG, Straub R, Roggan A & Felix R (1997) Magnetic resonance imaging--guided abdominal interventional radiology: laser-induced thermotherapy of liver metastases. Endoscopy 29(6): 577-83.

Vogl TJ, Muller PK, Mack MG, Straub R, Engelmann K & Neuhaus P (1999b) Liver metastases: interventional therapeutic techniques and results, state of the art. Eur Radiol 9(4): 675-84.

Vogl TJ, Straub R, Eichler K, Woitaschek D & Mack MG (2001) [Modern alternatives to resection of metastases--MR-guided laser-induced thermotherapy (LITT) and other local ablative techniques]. Ther Umsch 58(12): 718-25.

Vorbeck F, Cartellieri M, Ehrenberger K & Imhof H (2000) [Intraoperative navigation in paranasal sinus surgery with the Philips "Neuroguide" system]. Radiologe 40(3): 227-32.

Walsh TR, Weinstein JN, Spratt KF, Lehmann TR, Aprill C & Sayre H (1990) Lumbar discography in normal subjects. A controlled, prospective study. J Bone Joint Surg Am 72(7): 1081-8.

Weiger M, Pruessmann KP & Boesiger P (2002) 2D SENSE for faster 3D MRI. Magma 14(1): 10-9.

Weiner BK & Fraser RD (1997) Foraminal injection for lateral lumbar disc herniation. J Bone Joint Surg Br 79(5): 804-7.

Weishaupt D, Zanetti M, Hodler J, Min K, Fuchs B, Pfirrmann C & Boos N (2001) Painful Lumbar Disk Derangement: Relevance of Endplate Abnormalities at MR Imaging. Radiology 218(2): 420-7.

Wendt M, Busch M, Lenz G, Duerk JL, Lewin JS, Seibel R & Gronemeyer D (1998) Dynamic tracking in interventional MRI using wavelet-encoded gradient-echo sequences. IEEE Trans Med Imaging 17(5): 803-9.

White CS, Templeton PA & Hasday JD (1997) CT-assisted transbronchial needle aspiration: usefulness of CT fluoroscopy. AJR Am J Roentgenol 169(2): 393-4.

Wilppula E & Jussila P (1977) Spinal nerve block. A diagnostic test in sciatica. Acta Orthop Scand 48(5): 458-60.

Witt JD, Hall-Craggs MA, Ripley P, Cobb JP & Bown SG (2000) Interstitial laser photocoagulation for the treatment of osteoid osteoma. J Bone Joint Surg Br 82(8): 1125-8.

Woertler K, Vestring T, Boettner F, Winkelmann W, Heindel W & Lindner N (2001) Osteoid osteoma: CT-guided percutaneous radiofrequency ablation and follow-up in 47 patients. J Vasc Interv Radiol 12(6): 717-22.

Wohlgemuth WA, Wamser G, Reiss T, Wagner T & Bohndorf K (2001) In vivo laser-induced interstitial thermotherapy of pig liver with a temperature-controlled diode laser and MRI correlation. Lasers Surg Med 29(4): 374-8.

Wolf YG, Tillich M, Lee WA, Rubin GD, Fogarty TJ & Zarins CK (2001) Impact of aortoiliac tortuosity on endovascular repair of abdominal aortic aneurysms: evaluation of 3D computer-based assessment. J Vasc Surg 34(4): 594-9.

Yildiz Y, Bayrakci K, Altay M & Saglik Y (2001) Osteoid osteoma: the results of surgical treatment. Int Orthop 25(2): 119-22.

Yrjana SK, Katisko JP, Ojala RO, Tervonen O, Schiffbauer H & Koivukangas J (2002) Versatile intraoperative MRI in neurosurgery and radiology. Acta Neurochir (Wien) 144(3): 271-8.

Zeng Q, Xiong L, Jinkins JR, Fan Z & Liu Z (1999) Intrathecal gadolinium-enhanced MR myelography and cisternography: a pilot study in human patients. AJR Am J Roentgenol 173(4): 1109-15.

Zhang Q, Chung YC, Lewin JS & Duerk JL (1998) A method for simultaneous RF ablation and MRI. J Magn Reson Imaging 8(1): 110-4.